Technical Report

TR-10-42

Mass transfer between waste canister and water seeping in rock fractures

Revisiting the *Q*-equivalent model

Ivars Neretnieks, Longcheng Liu, Luis Moreno
Department of Chemical Engineering and Technology
Royal Institute of Technology, KTH

March 2010

Svensk Kärnbränslehantering AB
Swedish Nuclear Fuel
and Waste Management Co

Box 250, SE-101 24 Stockholm
Phone +46 8 459 84 00

SKB

ISSN 1404-0344
SKB TR-10-42

Mass transfer between waste canister and water seeping in rock fractures

Revisiting the *Q*-equivalent model

Ivars Neretnieks, Longcheng Liu, Luis Moreno
Department of Chemical Engineering and Technology
Royal Institute of Technology, KTH

March 2010

Summary

Models are presented for solute transport between seeping water in fractured rock and a copper canister embedded in a clay buffer. The migration through an undamaged buffer is by molecular diffusion only as the clay has so low hydraulic conductivity that water flow can be neglected.

In the fractures and in any damaged zone seeping water carries the solutes to or from the vicinity of the buffer in the deposition hole. During the time the water passes the deposition hole molecular diffusion aids in the mass transfer of solutes between the water/buffer interface and the water at some distance from the interface. The residence time of the water and the contact area between the water and the buffer determine the rate of mass transfer between water and buffer.

Simple analytical solutions are presented for the mass transfer in the seeping water. For complex migration geometries simplifying assumptions are made that allow analytical solutions to be obtained. The influence of variable apertures on the mass transfer is discussed and is shown to be moderate. The impact of damage to the rock around the deposition hole by spalling and by the presence of a cemented and fractured buffer is also explored. These phenomena lead to an increase of mass transfer between water and buffer.

The overall rate of mass transfer between the bulk of the water and the canister is proportional to the overall concentration difference and inversely proportional to the sum of the mass transfer resistances. For visualization purposes the concept of *equivalent flowrate* is introduced. This entity can be thought as of the flowrate of water that will be depleted of its solute during the water passage past the deposition hole. The equivalent flowrate is also used to assess the release rate of radionuclides from a damaged canister. Examples are presented to illustrate how various factors influence the rate of mass transfer.

Sammanfattning

Vi presenterar modeller för transport av lösta ämnen mellan vatten som strömmar i sprickigt berg och kopparkapslar som omges av en lerbuffert. Transporten genom en oskadad lerbuffert sker enbart med molekylär diffusion eftersom lerans hydrauliska konduktivitet är så låg att strömningen kan försummas.

I bergssprickorna och i eventuellt uppsprucket berg i depositionshålets väggar för det sipprande vattnet med sig lösta ämnen. Medan vattnet strömmar förbi leran hinner lösta ämnen från vattnet diffundera till lerytan och vidare in i leran. På samma sätt kan lösta ämnen, till exempel radionuklider från leran, hinna diffundera ut ett stycke i det sipprande vattnet innan det lämnar leran. Vattnets uppehållstid och kontaktytan mellan vatten och lera bestämmer hur mycket lösta ämnen som kan transporteras till eller från leran.

Enkla analytiska lösningar som beskriver materietransporten i sipprande vatten i sprickor presenteras. För mer komplicerade strömningsgeometrier görs förenklande antaganden som möjliggör enkla analytiska lösningar. Inverkan av sprickor med variabel apertur diskuteras och visas vara begränsad. Vidare diskuteras och modelleras inverkan av en zon av uppsprucket berg i depositionshålets väggar samt av att lerbufferten har cementerat och att det bildats en genomgående spricka i den. Dessa fenomen ökar materietransporten mellan kapsel och strömmande vatten.

Materieöverföringshastigheten mellan det sipprande vattnet och en kopparkapsel är proportionell mot koncentrationsskillnaden och omvänt proportionell mot summan av materieöverföringsmotstånden. Ett begrepp som sammanfattar och enkelt åskådliggör transporten kallas *ekvivalenta flödet*. Denna storhet anger vilket vattenflöde som kan bli utarmat på ett löst ämne alternativt vilket flöde som tar upp en halt av exempelvis en radionuklid som är lika med halten inne i en skadad kapsel. Vi presenterar olika exempel som illustrerar hur olika faktorer påverkar materieöverföringen.

Contents

1 Aims and scope

In SKB performance assessment the rate of solute transport to and from a canister is summarised in a term called the equivalent flowrate, Q_{eq}. One aim of the present report is to revisit the equivalent flowrate model and concept in order to assess its range of validity for calculating mass transfer of solutes between water seeping in a fracture that intersects a deposition hole and the copper canister inside the buffer.

Another aim is to try to quantify the impact of a number of phenomena and situations that can influence the overall mass transfer of solutes to and from the canister. These include the presence of a zone of damaged rock in the deposition hole, a cemented and fractured buffer, a degraded concrete at the bottom of the deposition hole, mass transfer resistance in copper corrosion products and other phenomena such as flow in variable aperture fractures and impact of the intersection angle of the fracture with the deposition hole and the flow direction.

We discuss the important assumptions on which the model is based, and under what conditions the model is expected to be valid. The treatment is limited to solute transport between the seeping water in fractures in the rock, in the buffer and damaged canister including the complications caused by rock and buffer damages.

Solute transport to and from the backfill in the tunnel is not treated but the basic ideas and equations can be used also to describe solute transport in a damaged zone around a tunnel and in fractures intersecting the tunnel.

2 Introduction and overview

The deposition holes for the fuel canisters may be intersected by one or more fractures with seeping water. As long as the buffer surrounding the canisters is intact water will not flow through the buffer at a rate of importance for solute transport to or from the canister. Molecular diffusion in the porous buffer carries solutes faster through the buffer than flow does because the hydraulic conductivity of the buffer is extremely low /Process report 2006/. There are two main processes that govern the rate of solute transport between the seeping water and the canister. In the buffer solutes migrate by molecular diffusion. In the seeping water transport is also by flow. Figure 2-1 illustrates the three main paths by which nuclides that escape through a little hole in the canister can migrate to the seeping water in the fractures in the rock.

It has been found that under expected repository conditions the resistance to solute transfer between the seeping water and the buffer could be considerably larger than that in the buffer. This can limit the overall rate of mass transfer. A study of the governing mass transfer mechanisms between the seeping water in a fracture and the buffer resulted in a very simple model /Neretnieks 1979/ by which the rate of solute exchange between water and buffer can be estimated. The model has been used in the SKB safety analysis since KBS-2 in 1978. The model has also been used to calculate the transport of corrosive agents to the canister.

The model is based on mathematical descriptions of established and well-known physical processes. In performance assessment calculations the water flowrates and velocity in the fractures intersecting a deposition hole are obtained from fracture network hydraulic modelling. This is not discussed here. The description of solute transport by molecular diffusion in the water is based on Fick's first and second laws. A number of simplifying assumptions were used to derive the original model /Neretnieks 1979/. For example an ideal interface between the buffer and rock was assumed, i.e. no rock spalling and no excavation damaged zone (EDZ) were accounted for. The fracture was modelled as having smooth parallel walls and no fracture infill. It was also assumed that the flowrate and flow direction do not vary in time. Furthermore, the mass transfer rate is assumed to have reached a steady state. These and other assumptions will be discussed and what uncertainties they may give rise to. These uncertainties will be related to the variations of mass transfer rates that are expected due to the large span of flowrates known to exist between different fractures and the likewise large difference in apertures between different fractures.

In this report we extend the model to solute transport in zones where the rock has been subject to so high stresses that spalling has occurred in the walls of the deposition hole. The damaged zone may have a much higher hydraulic conductivity and porosity than the intact rock. The flowrate and residence time of the water in contact with the buffer can be larger than what can be expected in one or a few fractures that intersect the deposition hole. This could lead to considerably larger rates of solute transport to or from the buffer.

When there is a potentially large mass transport rate between seeping water and buffer (small resistance) the overall rate may be limited by the solute transport through the buffer. This is also addressed in the report.

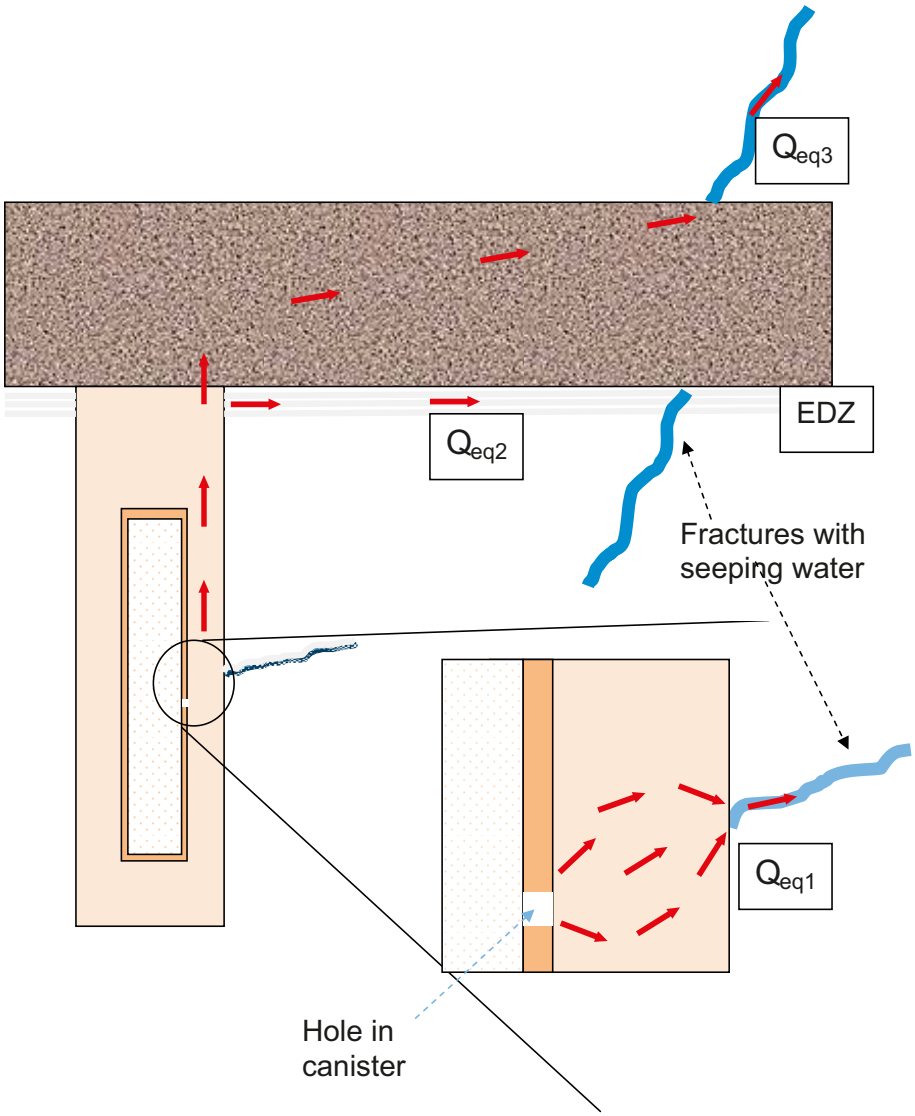

Figure 2-1. *Illustration of a leaking canister and the three paths the nuclides migrate.*

2.1 The concept and use of the notion of "equivalent flowrate" Q_{eq}

The term equivalent flowrate was introduced to facilitate understanding of how much solute (corrosive agent or nuclide) could be transported to or from the canister by the water seeping in the rock.

The basic idea is to assess the rate of solute transport to or from a canister. For visualization purposes it is expressed as the flowrate of water that would be depleted of (filled with) its solute when the water passes the deposition hole. The rate of transport is proportional to the driving force, here expressed as the concentration difference and inversely proportional to a resistance $R^{overall}$ to solute transfer, i.e. we can write,

$$N = Q_{eq}^{overall}(c_w - c_o) = \frac{1}{R^{overall}}(c_w - c_o) \tag{2-1}$$

or, in view of the fact that the overall resistance can be made up of a sum of resistances in the barriers through which the solute has to pass in series,

$$N = \frac{1}{\sum_i R_i}(c_w - c_o) = \frac{1}{\sum_i \frac{1}{Q_{eq,i}}}(c_w - c_o) \tag{2-2}$$

N is the rate of exchange of a solute between the seeping water having a concentration c_w to a body (canister) that maintains its concentration at c_o (for example c_o equal to zero if the corrosive agent immediately reacts with the copper canister). The ingress of a corrosive agent is illustrated in Figure 2-2.

The same expression can be used for release of a nuclide from the canister to the passing water. Then c_o could be the nuclide concentration inside the canister and c_w the concentration in the approaching water. The latter would commonly be zero.

The equivalent flowrate Q_{eqW} or its inverse, the resistance R_w, for the transfer from the water seeping in the fractured rock to the outer surface of the buffer can be determined by assessing how far out in the flowing water the solute can be depleted by diffusion during the time the water is in contact with the buffer. When the water ceases to be in contact with the buffer it has been depleted of a given mass of solute. This is obtained by modelling the flow and solute transport by well-known relations (Darcy flow and Fick's second law).

The solute encounters a number of transport resistances in series. For example in the canister defect scenario for transport from the fuel to the seeping water a nuclide has to diffuse from the fuel through a hole in the canister to the clay buffer, then from the exit of the hole in the canister out into and through the buffer to reach the seeping water in the fracture in the rock. As the nuclide approaches the fracture in the rock it will have to find the narrow fracture. This can also be expressed as a resistance. All these resistances can be expressed as inverse of the corresponding equivalent flowrates. The combined effect of all these resistances in series can be found by adding all the resistances as shown in Equation 2-1 and 2-2.

Expressing the transport in this way can be used to visualize which part of the system has the largest impact on the transport. The smallest $Q_{eq,i}$ (largest of the resistances in series) will have most impact on limiting the rate of transport to and from the canister. In the following sections the resistances and equivalent flowrates for the different barriers are described.

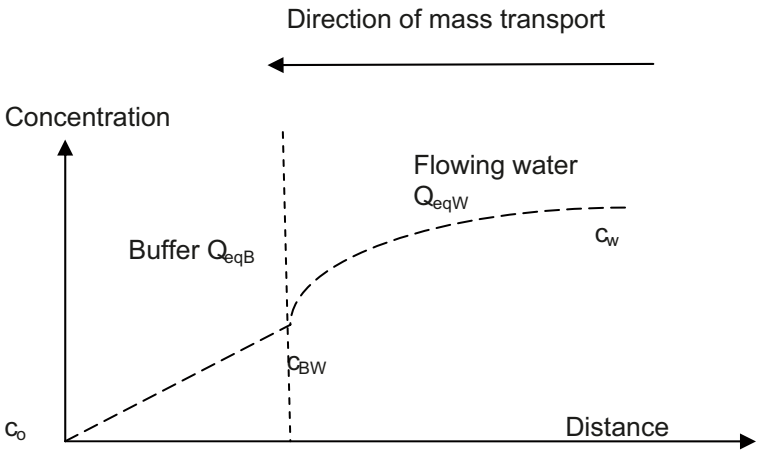

Figure 2-2. *Solute transport from bulk water to interface between water and buffer and further transport by diffusion through buffer to canister surface.*

3 Mass transfer between water in fractures to and from the canister

3.1 Overview of the mass transfer from water seeping in the fractured rock to the buffer and further through the buffer to the canister surface

In this chapter we describe the underlying physics and present simple analytical solutions for constant aperture fractures intersecting the deposition hole at right angles. The model is extended to apply also for fractures intersecting the deposition hole at an arbitrary angle also using analytical solutions. Processes in rough and variable aperture fractures are modelled by numerical methods and it is shown that the simple analytical solution can be used also for variable aperture fractures.

A solute carried by the seeping water in a fracture in the rock will diffuse in the directions where the solute concentration is lower. It is first exemplified by a corrosive agent carried by the water, where the solute when it reaches the canister surface reacts rapidly and attains a concentration equal to zero. The solute diffuses from the bulk of the water toward the interface between water and buffer. In a steady state situation the concentration at the buffer/water interface is constant and lower than that in the approaching water. In a fracture the cross section for diffusion is set by the fracture aperture. For a given flowrate the water velocity is higher in a narrow fracture than in a fracture with a larger aperture. The residence time for water passing the buffer interface will be small as will the contact area for a narrow fracture. Both these factors make the mass transfer small in a narrow fracture because the time for the species to diffuse from the bulk of the water to the buffer is small as is the transfer area. The fracture aperture will have a strong influence on the water velocity and residence time in contact with the buffer.

A complication is introduced when the rock nearest the buffer is damaged for example due to spalling. The damaged rock may have a large number of fractures, which increases the contact area between the seeping water and the buffer. Furthermore the porosity of the damaged zone may be much larger that of the undamaged rock, allowing the water to have a much larger residence time at the buffer surface. This allows more solute to reach the buffer surface. In addition, due to the higher conductivity, the damaged rock will “draw in” more water than the fracture in an undamaged rock. This also increases the rate of mass transfer.

Solute that reaches the buffer surface diffuses into the buffer where it spreads out from the mouth of the narrow fracture(s) and thus has a much larger cross section area to diffuse through than the narrow fracture in the rock allowes The diffusion resistance in the buffer will set an upper limit on the mass transfer, given that the other resistances become small due to spalling damages.

Solute transport in the opposite direction of for example escaping nuclides, i.e. from the canister towards the seeping water, is subject to exactly the same processes, and the relations that will be described apply identically to both transport directions. Nuclides escaping from the interior of the copper canister will have to pass through the damage in the copper shell and an additional resistance can be considered if the damage is a narrow hole.

In this report the five regions are treated and models presented on how to assess the transport resistances in

- Seeping water in a fracture
- Seeping water in rock damaged by spalling
- Seeping water in degraded concrete at the bottom of the deposition hole
- Buffer
- Narrow hole through copper canister

The regions will be treated in this order. To help the reader get a feeling for mass transfer resistances and mass transfer rates the concept of an equivalent flowrate, Q_{eq} is used. In chemical engineering

terminology it is the product of the mass transfer coefficient and the contact area. It is the inverse of the resistance R to mass transfer. In the present situation there are several elements coupled in series through which the solute has to migrate to or from the canister. In one case also parallel paths are considered.

The Q-equivalent shows the transport capacity for a given concentration difference. It is a fictive flowrate that allows Q_{eq} m^3/s of approaching water to deliver solute in it to the canister surface or for an escaping nuclide to escape from the interior of the canister to the seeping water. Every barrier can be assigned its own resistance and thus equivalent flowrate. This facilitates the comparison of the barriers. The larger the Q_{eq} is for a barrier the less resistance it offers for mass transfer.

3.2 The basic concepts of the Q_{eq} model for water seeping in a fracture

Figure 3-1 shows a canister deposition hole intersected by a fracture with seeping water seen from the side and from above. The water has to flow around the hole because the buffer has so low hydraulic conductivity that it will hinder water flow through it.

The mass transfer is illustrated with a nuclide that has penetrated through the buffer and is released into the water. Exactly the same processes will govern a solute that is carried by the water and migrates into buffer from the water. This would apply to a corrosive agent e.g. sulphide.

The nuclide has reached and maintains a steady state concentration c^i_{BW} at the interface between buffer and water. Under repository conditions the flow is laminar and the nuclide moves by molecular diffusion into the water. It diffuses further and further out into the water as the water moves along the buffer/water interface. The water picks up more and more nuclide along its path around the deposition hole. By the time it leaves the buffer surface and flows downstream it carries an amount of nuclide. From diffusion theory we can determine the flowrate of nuclide, N [moles/s], that the water has picked up and carries away.

For a nuclide i the migration rate from the buffer/water interface to the approaching water that contains no nuclide is

$$N_i = Q_{eq,i}(c^i_{BW} - c^i_w) = Q_{eq,i}c^i_{BW} \qquad (3\text{-}1)$$

N_i is the flowrate of nuclide i.

It may be noted that the diffusion coefficients of the nuclides and the other solutes of interest here are very similar and that $Q_{eq,i}$ will differ little between species. Therefore in the following we omit index i.

Figure 3-2 illustrates how the concentration of the species increases as the water passes the buffer. Downstream of the deposition hole only a narrow stream contains the solute. In this example the

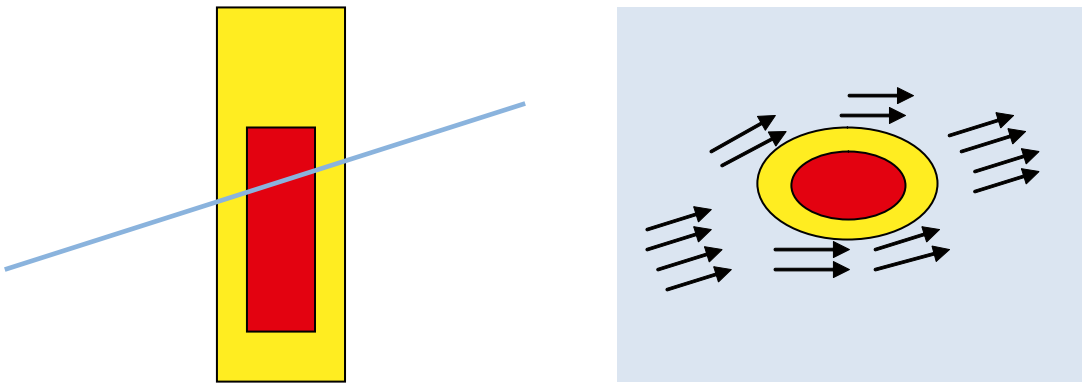

Figure 3-1. *Canister deposition hole with tight buffer intersected by a fracture with flowing water. Water flows around the buffer.*

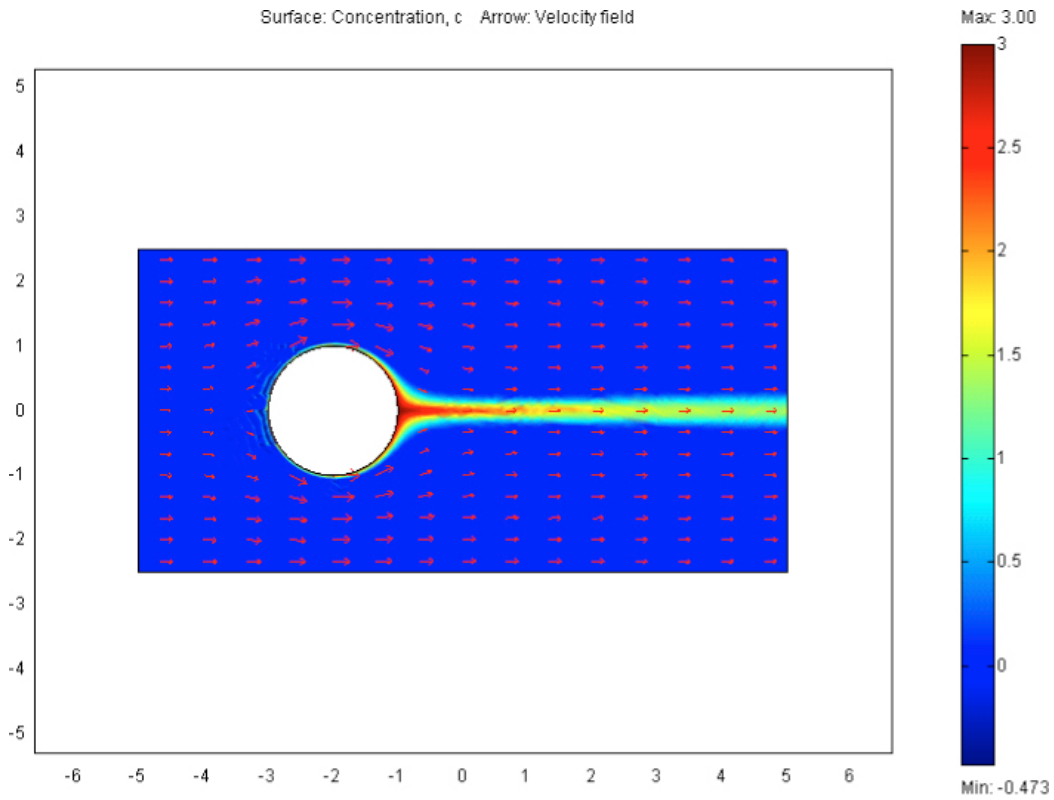

Figure 3-2. *Groundwater flows in the intersecting fracture around the deposition hole. A solute is released from the buffer and diffuses into the groundwater. The concentration is shown by the colour surface plot and the groundwater velocity by the arrow plot.*

residence time of the water was short and the solute had only time to diffuse a short distance out into the water. A longer residence time would have allowed the solute to diffuse further out.

This conceptual approach to model solute transfer between an interface and a flowing fluid has been used in a multitude of chemical engineering applications and other areas of heat and mass transfer for a very long time. A thorough description can be found in /Bird et al. 2002/.

3.3 Water flowrate, velocity and residence time

We have experienced that to understand the concept of the equivalent flowrate and the mechanisms underlying it a short description of the mechanisms that govern it has been helpful. We therefore outline the basic ideas and processes and give an approximate expression before presenting an exact solution.

In this section the migration of a solute coming from the surface of the buffer diffuses into seeping water that has no solute is described. It has been found that this is conceptually somewhat easier to grasp than the opposite direction although it is entirely equivalent.

We assume that the water flowrate and velocity u in the fracture, far from the deposition hole, is known. The velocity near the deposition hole increases as the water is forced to flow around the buffer. A fair approximation of residence time for the water passing the hole is obtained by the time it takes for the undisturbed water velocity u to travel a distance equal to the diameter of the deposition hole.

$$t_{res} = \frac{2r_h}{u} \tag{3-2}$$

where r_h is the radius of the deposition hole.

During the time the water has been into contact with the buffer, travelled along the interface and left it, the water has been exposed to the concentration c_{BW} at the buffer/water interface. During this time the solute has diffused further and further out into the water. A concentration profile builds up. The situation can be approximated by diffusion into stagnant water exposed at one boundary to concentration c_{BW} during t_{res}.

From diffusion theory we have that the mean penetration depth η_{mean} of the solute can be determined by integrating the concentration profile from the surface to infinity /Bird et al 2002, p 621/. That will be the distance from the surface of the buffer, which the solute has diffused from the buffer and will have attained the concentration c_{BW}. It is /Neretnieks 2006a/,

$$\eta_{mean} = \sqrt{4D_w t_{res}/\pi} = 1.13\sqrt{D_w t_{res}} \tag{3-3}$$

D_w is the diffusion coefficient of the solute in water. It is different for different solutes but is typically in the range 1 to $3\cdot10^{-9}$ m^2/s for small molecules and ions in water at temperatures expected at repository depth. Considering the uncertainties in determining the water velocity and fracture aperture it is deemed permissible to approximate it as being independent of solute. A value of $1\cdot10^{-9}$ m^2/s will be used in the examples.

In addition, it is emphasised that in writing Equations 3-2 and 3-3 the viscous boundary layer caused by the presence of the buffer is considered to be thin compared with the boundary layer where diffusive mixing of solute with water occurs. This is justifiable by accounting for the fact that the velocity in the fracture is determined by the friction against the walls of the fracture except very near the interface with the buffer. There the velocity profile is also influenced by friction against the buffer. Thus at a distance on the order of the fracture aperture from the buffer the mean velocity in an even aperture fracture is constant.

Having Equation 3-3, the flowrate of water that has gained the concentration c_{BW} is given by,

$$Q_{eq} = 2u\delta\eta_{mean} = 2.26\delta\sqrt{D_w 2r_h u} \cong 3.2\delta\sqrt{D_w r_h u} \tag{3-4}$$

δ is the fracture aperture. The factor 2 comes from the fact that fluid passes both sides of the hole.

Should the approaching water already have a concentration c_a, the equivalent flowrate means the flowrate that has increased its concentration from c_a to c_{BW}.

3.4 Exact solution for mass transfer from a circular cylinder

The simple expression above, Equation 3-4, is qualitatively correct but as diffusion in the flow direction as well as the velocity differences between the streamlines adjacent to the deposition hole have been neglected and the curvature has been straightened out, the constant in Equation 3-4 is not correct. The exact solution is presented below. The derivation of it can be found in /Chambré et al. 1982/. Chambré derived an exact solution to the problem also including the instationary phase where the solute diffuses into the flowing water and gradually builds up the final steady state profile. At steady state and valid for Pe>4 the result is

$$Q_{eq} = 8\delta D_w\sqrt{\frac{Pe}{\pi}} \cong 4.51\delta D_w\sqrt{Pe} = 4.51\delta\sqrt{D_w r_h u} \tag{3-5}$$

The Peclet number, Pe, is defined as

$$Pe = \frac{u r_h}{D_w} \tag{3-6}$$

Equation 3-5 gives a 40% higher value than Equation 3-4. For the Pe to be larger than 4 the water velocity must be larger than 0.14 m/yr. It is hence justified that Pe>4 holds in most conditions of interest to the performance assessment of repositories for spent nuclear fuel.

In practice, the Peclet number can be interpreted as the ratio of advective transport to that by diffusion.

For illustration purposes we take that the water velocity is obtained from the transmissivity T and hydraulic gradient i in the fracture. In performance assessment, the velocity is obtained from the results from solving the flowrates in all fractures in the fracture network.

$$u = \frac{Ti}{\delta} \tag{3-7}$$

which, when introduced in Equation 3-5 gives

$$Q_{eq} = 4.51\sqrt{TiD_w\delta r_h} \tag{3-8}$$

Figure 3-3 shows Q_{eq} as a function of fracture transmissivity for gradients 0.001, 0.01 and 0.1 m/m for a diffusivity D_w=10^{-9} m^2/s. The range of data are selected to cover high transmissivity fractures potentially intersecting deposition holes and very large gradients that possibly could occur during inland ice advance and withdrawal.

Figure 3-3 shows that the seeping water can only carry an amount of solute that can be dissolved in at most a few litres of water per year even under high gradients and in fractures with large transmissivities.

3.5 Variable aperture fractures and fracture roughness

The above descriptions of flow and solute transport were based on an idealized description of the fracture as being a slit between two smooth surfaces. Real fractures have variable aperture and the two surfaces are in contact in many locations to support and transmit the rock stresses. The open parts of the fracture may be in contact with other open parts and form an essentially two dimensional network that allows the formation of long connected paths along which the water can flow. We call these paths channels but recognize that the flow can seek out different paths when the hydraulic gradient direction changes. In the discussion below we do not account for the possible presence of permanent channels that may have formed by mineral dissolution or precipitation because we have not found data to quantify such channels or the presence of fault gauge or infill.

/Liu and Neretnieks 2005b/ studied flowrates and solute transport to and from a canister deposition hole in variable aperture fractures. The aperture was taken to be log normally distributed, which is supported by experiments. Both Gaussian and fractal distributions were used to relate how aperture in one location is correlated to that in other points at some distance.

Figure 3-4 shows an example of a Gaussian variable aperture fracture with log normal aperture distribution and a correlation length equal to 10% of the fracture size.

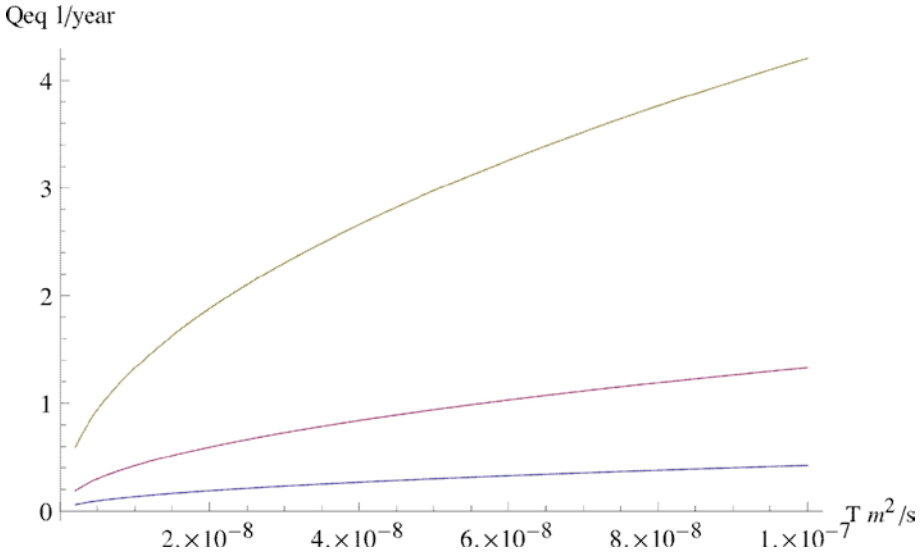

Figure 3-3. *Equivalent flowrate as a function of transmissivity for gradients 0.001 (lowest curve), 0.01 and 0.1 m/m in an 0.1 mm aperture fracture, r_h=0.875 m and D_w =10^{-9} m^2/s.*

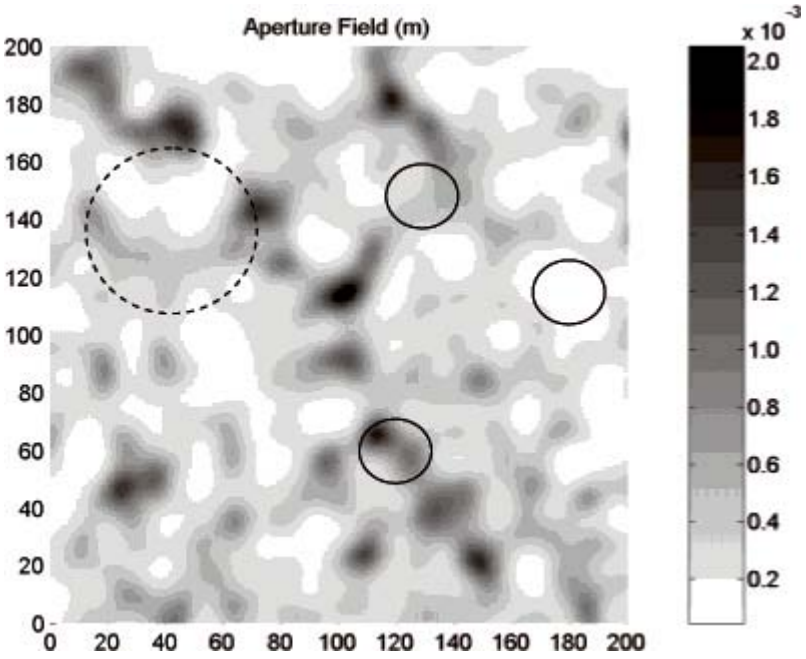

Figure 3-4. *A realization of the aperture spatial distribution in the fracture plane The fracture is portioned into 200 times 200 equal size elements, and the arithmetic mean in the log normal distribution $\mu=3.5\cdot10^{-4}$ m, with standard deviation $\sigma=1.5\cdot10^{-4}$ m. The correlation length is 1/10 of the fracture dimension, i.e. 20 size elements.*

The small circles indicate three possible different positions of a deposition hole. The rightmost small circle is located in an essentially tight area and will not be exposed to much flow. The upper small circle will have a possible flowpath on its right side and the lower circle could practically cut off a potentially high flowrate path. These three circles representing the diameter of a deposition hole are comparable to the correlation length. Such deposition holes could essentially be surrounded by very tight or very open sections. If the correlation length is much smaller than the deposition hole it is likely to be in contact with potentially flowing channels as illustrated by the large circle, which is about two and a half times larger than the correlation length.

The size of the deposition hole relative to the correlation length can be expected to influence the flowrate that comes into contact with the deposition hole and therefore the rate of mass transfer between the seeping water and the buffer.

A number of simulations were performed where the flow field in the variable aperture fractures was solved numerically. The fracture size was 10×10 m with a deposition hole with radius 0.875 m in the centre of the fracture. The correlation length or the cross over dimension was varied between zero and 50% of the fracture dimension. The arithmetic mean aperture was $\mu=3.5\cdot10^{-4}$ m and the standard deviation σ was varied between 0 and 0.8 μ. The roughness is defined here as σ/μ.

The probability density function of aperture refers here to what is sometimes called the mechanical aperture δ_m. It is the aperture that could be measured by a ruler.

The hydraulic aperture δ_h is a term used to designate the size of an equivalent smooth walled slit that has the same hydraulic transmissivity as the real fracture. The hydraulic aperture is used in the cubic law relation between hydraulic aperture and transmissivity.

Assuming that the cubic law is valid locally the hydraulic aperture can be obtained as the geometric mean of a given distribution of mechanical apertures, /Keller 1997/. It is always smaller then the mechanical aperture. This implies that a rough walled fracture always will have a lower hydraulic transmissivity than a smooth walled fracture given the same mean mechanical aperture. The flowrate will thus be smaller in a rough walled fracture with the same mean mechanical aperture as a smooth walled slit. This will also influence the equivalent flowrate. This can be seen in Figure 3-5 where the normalized equivalent flowrate decreases with increasing roughness, σ/μ. For constant aperture

fracture (i.e. a parallel plate fracture with an aperture determined by the hydraulic aperture of the rough walled fractures), on average Q_{eq} decreases by 40% for a roughness of 0.8 compared to a smooth fracture.

Figure 3-5 also shows that for different realizations of the stochastic fractures that the spread in Q_{eq} increases with increasing roughness. Each point in the figure represents the average of 50 realizations. Results are shown for cross over dimensions from zero up to 0.5 of the fracture size. The cross over dimension is the longest wavelength that has significant amplitude, and conceptually it is equivalent to correlation length but used for fractal fractures /Liu and Neretnieks 2005a/. The correlation length is used for description of Gaussian fractures, the mathematical model of which is very different from that of fractal fractures.

The error bars represent plus minus one standard deviation for each correlation length. It is seen that the standard deviation increases with correlation length as well as with roughness. The weak gray lines give the bounds for two standard deviations of the whole ensemble. A detailed analysis of the data reveals that a Normal distribution reasonably well describes the data.

Gaussian aperture size distribution gives very similar results.

If one wishes to use a stochastic approach to assess the equivalent flowrate in a variable aperture fracture the following expression can be used.

$$p\left(\frac{Q_{eq}}{Q_{eq,\sigma=0,b=\mu}}\right) = N[1, C_{eq}\frac{\sigma}{\mu}\frac{l_c}{L}] \tag{3-9}$$

Here p is the probability function, Q_{eq} is the stochastic value, $Q_{eq,\sigma=0,b=\mu}$ is the value for a smooth fracture with an aperture μ. l_c is the correlation length, L is the length of the fracture in the direction normal to fluid flow. N denotes the Normal distribution function with mean 1 and standard deviation $C_{eq}\frac{\sigma}{\mu}\frac{l_c}{L}$. C_{eq} is a constant that is between about 2 and 7 for both Gaussian and fractal fractures.

Considering that the four entities σ, μ, l_c and L are probably poorly known and C_{eq} can vary one possible choice would be to use the analytical solution directly based on measured or estimated values of transmissivity and aperture without adding any further stochastic component. The underestimation of Q_{eq} is then less than a factor two even for the roughest fractures and is often much less than this.

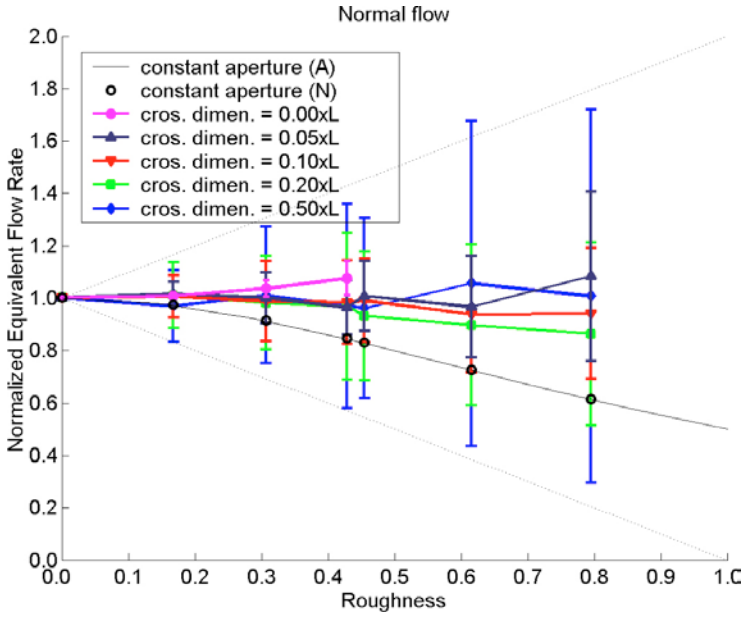

Figure 3-5. *An example of normalized equivalent flow rates for flow through a single fracture of the fractal type with μ=3.5·10^{-4} m and size L = 10 m compared to that through a smooth parallel plate fracture. A and N stand for analytical and numerical results.*

3.6 Fractures intersecting the deposition hole at an angle

The above analysis was based on fractures that intersect the deposition hole at right angles. Fractures may intersect the deposition hole at all angles, which will lead to an increase in the contact area between the seeping water and the buffer. /Liu and Neretnieks 2004/ developed exact and approximate solutions for Q_{eq} for such cases.

Following the studies of /Chambré et al. 1982/ for the case where the flow is taken normal to the axis of the canister, the equivalent flowrate for the solute transport from the canister by diffusion and advection through an infinite large fracture with parallel plate geometry is given by Equation 3-5 shown earlier.

To be generalized to other cases, an equivalent radius for the inclusion should be used in place of r_h in the Peclet number. This equivalent radius can be defined as r_s, as given by Equation 3-10, and the radius of an equivalent circular cylinder that has the same area as that of the inclusion is

$$r_s = \sqrt{\frac{S_i}{\pi}} \tag{3-10}$$

where S_i is the area of the intersection.

The Peclet number should also be modified by a shape factor f_s that explicitly accounts for the difference in the shape of the inclusion /Liu and Neretnieks 2004/.

With these considerations, we may generalize the Peclet number as,

$$Pe = \frac{ur_s}{D_w} f_s \tag{3-11}$$

where the shape factor, is given by,

$$f_s = \frac{l + w}{2\sqrt{lw}} \tag{3-12}$$

w is width of the inclusion in the direction normal to fluid flow and l is the length of the inclusion in the direction parallel to fluid flow.

Generalization of the Peclet number in this manner makes Equation 3-5 applicable to cases where the flow may be taken normal, inclined or parallel to the axis of the canister, as suggested by numerical validations. The analytical solutions, obtained by Equation 3-5 and 3-10 to 3-12, agree extremely well with the numerical solutions, obtained by solving the transport equation for conservation of the solute mass by FEMLAB®, /Liu and Neretnieks 2004/. The difference between the simulated and the analytical solutions is at most 1%. The above equations provide a simple means to quantify the mass transfer from the canister by diffusion and advection through a single fracture that intersects the canister at arbitrary angles.

For a KBS-3 deposition hole with radius 0.875 m the equivalent flow rate increase would be a factor of 1.10 in the case of inclined flow with an angle of 45°, and a factor of 1.44 higher for a vertical intersection. However, a vertical fracture will also intersect the deposition tunnel. This leads to streamline disruption by the tunnel that is not included in the analysis. This effect would decrease the equivalent flowrate. In practice one might expect no more than a few tens of % increase of Q_{eq} at most.

Referring to the paragraph above, the uncertainty in flow directions is thus marginal in the safety and performance assessment of a deep repository for spent nuclear fuel.

4 Mass transfer in a damaged rock wall in the deposition hole and in a degraded concrete bottom plate

4.1 Overview of damage exemplified by spalling

In this chapter we account for the presence of damaged zones in the deposition hole, which leads to draw-in of more water into the zone and to a longer residence time in contact with the buffer. An analytical model to allow for this is presented and examples are shown how this may increase the rate of solute transport.

It is envisaged that the tunnels will be aligned in the direction of highest horizontal stress. Any spalling damage will occur on the sides of the deposition hole perpendicular to that direction. This is illustrated in Figure 4-1. In experiments at Äspö HRL in a full size deposition hole the damaged zone was wedge formed about 50 cm wide and 20 cm deep and extended along the entire hole length /Andersson 2007/. The rock fragments were shaped like flat thin sheet like double pyramids, as schematically shown later in Figure 4-3. The longer dimensions were aligned parallel to the length of the deposition hole. Their thickness to length or width was about 1/10. The largest fragments were up to 50 cm and the number of fragments increased with decreasing size. The fragments were collected. Their size, length to width and thickness to length was measured down to sizes of about 5 cm. Smaller fragments were size classified by sieving. This information was used to estimate particle size distribution and the surface area of the fragments in different size classes.

The particle shape was used to estimate the tortuosity for flow and solute transport in the damaged zone and the size and surface area distributions can be used to assess hydraulic properties of the damaged zone /Neretnieks and Andersson 2009/.

4.2 Flow to and in a damaged zone

From the measurements of the rock fragments it can be deduced that the hydraulic conductivity of the damaged zone is likely to be so high that it will not offer much flow resistance compared to the other resistances. On the contrary it can be taken to have no flow resistance at all for the purpose of calculating the water flow in the zone. The water flowrate will be determined by the transmissivity of the fracture(s) intersecting the damaged zones. The flow conditions in a damaged zone intersected by a fracture have been described and analyzed by /Neretnieks 2006b/. In that analysis the scenario chosen was that a fracture intersects the deposition hole at some angle and that water is drawn in on one side of the intersection with the damaged zone and out on the other. It was assumed that the hydraulic conductivity of the zone was very large and the transmissivity of the fracture limits the flowrate through the zone. It was shown that the water spreads out upward and downward along the zone in its passage. The water is effectively in contact with the buffer over only a fraction of the damaged zone. The residence time is also shorter than if it had access to all the pore space in the zone.

Here this situation is extended to a case where there also is a conductive region at the bottom of the deposition hole. This could be caused by chemical degradation of the concrete foundation at the bottom of the hole, which is cast to ensure that the bottom is level and smooth.

Figure 4-1 illustrates how water can flow into the zone, down to the bottom of the deposition hole where the concrete bottom plate has been degraded and up the zone on the other side of the hole. The same approach can be used to account for the presence of any excavation damaged zone at the bottom of the deposition tunnels.

The water flowing in the damaged zones will have a longer contact time with the buffer than what it would have without the presence of the damaged zones. In the example described in Section 4.6, the water enters the damaged zone flows downward until it reaches the bottom of the deposition hole with the degraded porous concrete, flows through this and then upward in the opposite zone. As the

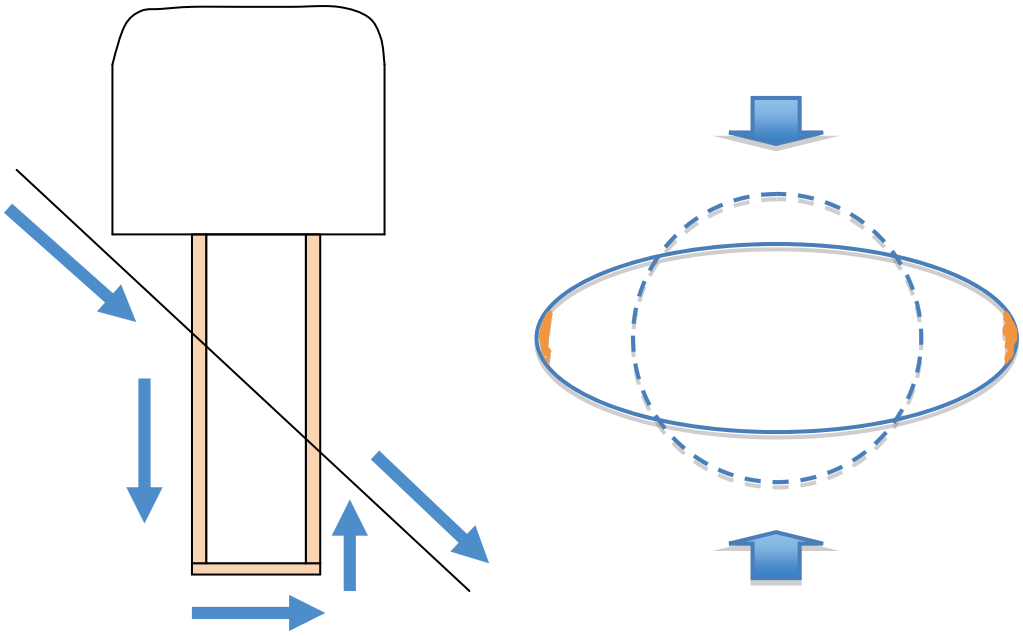

Figure 4-1. *Illustration of a deposition hole with spalling damage and a fracture intersecting the hole. Arrows indicate possible flowpaths. The right picture shows how spalling occurs, marked orange, when the hole is compressed by rock stresses. The width of the zone as seen in the right hand figure is denoted W later.*

mass transfer properties and geometries in the zone and the concrete are very different we describe the mass transfer as if it takes place in two different parallel paths that do not influence each other. This is an approximation we make in order to derive simple expressions. It introduces some error but this is small compared to other uncertainties.

First the mass transfer through the zone and in the concrete are treated. Then the mass transfer through the buffer to/from the zone and concrete are described. Finally, in a later example the two resistances in each path are added giving the mass transfer through each of the, supposedly, independent paths.

4.3 Mass transfer between water in a damaged zone and buffer

The water that flows in the damaged zone around the canister will carry a solute migrating to the buffer or take up a solute from the buffer by molecular diffusion. The longer the water is in contact with the buffer the more solute can be transferred. We use a simplified model to describe the system and to quantify the rate of mass transfer and the equivalent flowrate. Figure 4-2 shows how the system is conceptualized and simplified. The damaged zone and rock curvature are straightened out and the flow is now linear. The damage is approximated by a rectangular cross section. The distance along the flow direction is designated by x and the distance from the buffer surface is y. First we describe a case where the mass transfer from the degraded concrete is neglected and only that from the water in the damaged zone(s) is accounted for. However, the zones are connected as in Figure 4-1.

If only advection in the x-direction and molecular diffusion in x- and y-directions are active the solute concentration over time and in space in the water can be described by the partial differential equation

$$\frac{\partial c}{\partial t} + u\frac{\partial c}{\partial x} = D_{px}\frac{\partial^2 c}{\partial x^2} + D_{py}\frac{\partial^2 c}{\partial y^2} \qquad (4\text{-}1)$$

We will later also discuss the impact of dispersion caused by the meandering paths between the rock fragments in the spalling zone. When dispersion adds to the mixing Equation 4-1 still can be used as an approximation but the diffusion coefficients are then to be interpreted as dispersion coefficients.

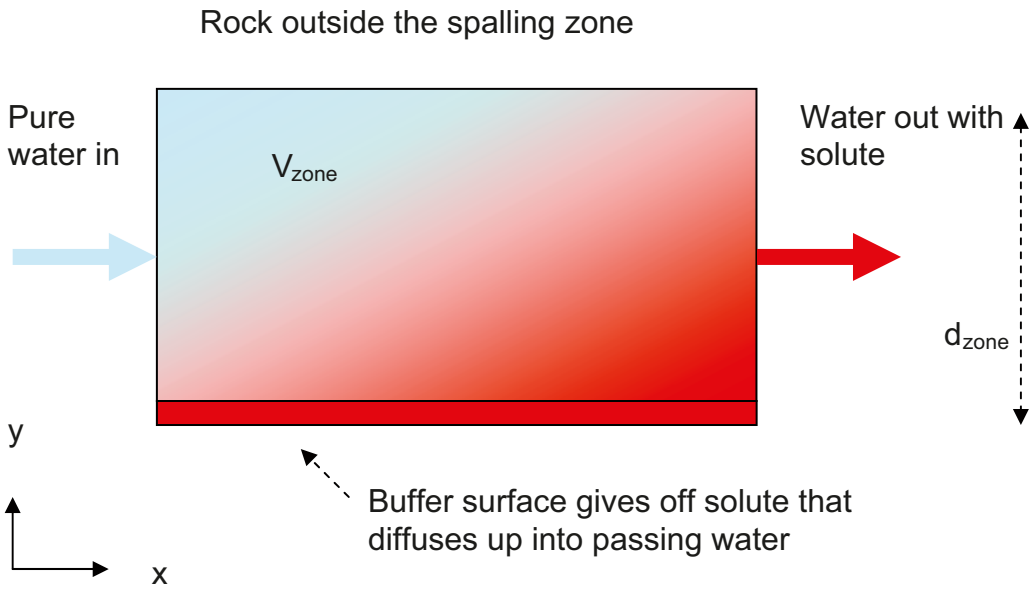

Figure 4-2. *Water flowing through the damaged zone is contaminated by a solute released from the buffer surface.*

The diffusivity in the x-direction is considerably larger than in the y-direction because in the x-direction the flowpaths are essentially parallel to the nearly flat fragments but in the y-direction the migration paths are strongly zigzag formed, as illustrated in Figure 4-3. This reduces the rate of diffusion in the y-direction by about a factor of 100 compared to that in straight paths /Neretnieks and Andersson 2009/, see also Section 4.4.

Assuming plug flow, i.e. that the velocity is constant over *y*, this equation can be simplified as we only consider a stationary case when the concentration does not change over time but only in space.

Then $\frac{\partial c}{\partial t}$ =0 and

$$\frac{\partial c}{\partial t_{res}} = D_{px}\frac{\partial^2 c}{\partial x^2} + D_{py}\frac{\partial^2 c}{\partial y^2} \qquad (4\text{-}2)$$

where t_{res} is x/u. Thus only the residence time of the water need to be accounted for.

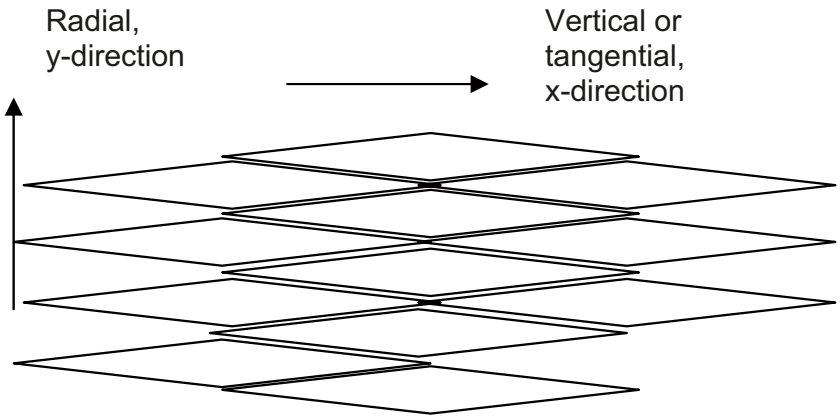

Figure 4-3. *Arrangement of the rock fragments and flow directions.*

A further simplification is made by neglecting the diffusion in the x-direction. This is reasonable because the diffusion in the x-direction in relation to the distance squared is much smaller than that in the y-direction as can be seen by using the transforms $X = \frac{x}{x_o}$ and $Y = \frac{y}{y_o}$. The diffusivity in the y-direction is about 100 lower than that in the x-direction. See section 4.4. The distance in the x-direction x_0 is about 10 m and that in the y-direction y_0 is about a tenth of a metre as will be shown in the examples below. This means that $\frac{D_{py}}{y_o^2}$ is about two orders of magnitude larger than $\frac{D_{px}}{x_o^2}$ and we can neglect the diffusion in the x direction in comparison to that in the y direction.

$$\frac{\partial c}{\partial t_{res}} = \frac{D_{px}}{x_o^2}\frac{\partial^2 c}{\partial X^2} + \frac{D_{py}}{y_o^2}\frac{\partial^2 c}{\partial Y^2} \cong \frac{D_{py}}{y_o^2}\frac{\partial^2 c}{\partial Y^2} \tag{4-3}$$

The errors introduced are deemed to be marginal compared to those caused by the geometrical simplifications and other assumptions. The merit of the simplifications is that some very simple analytical expressions can be derived suitable for stochastic simulations. The simple expressions also give a good insight into the dominating mechanisms and parameters.

Then, the equation to solve is

$$\frac{\partial c}{\partial t_{res}} = D_{py}\frac{\partial^2 c}{\partial y^2} \tag{4-4}$$

with initial and boundary conditions

$c = 0$ at $t_{res} = 0$ (4-5)

$c = c_{BW}$ at $y = 0$ (4-6)

$$\frac{dc}{dy} = 0 \quad at \quad y = d_{zone} \tag{4-7}$$

In writing Equation 4-7, we have neglected further diffusion into the rock beyond the spalling damage. The solution for the outlet concentration profile is /Bird et al. 2002, p 377/

$$\frac{c}{c_{BW}} = 1 - 2\sum_{n=0}^{\infty}\frac{(-1)^n}{(n+1/2)\pi}e^{-\frac{(n+1/2)^2\pi^2 D_{py}t_{res}}{d_{zone}^2}}Cos((n+1/2)\frac{\pi(d-y)}{d_{zone}}) \tag{4-8}$$

The mean concentration c_{mean} is obtained by integration over the distance from $y = 0$ to $y = d_{zone}$.

$$\frac{c_{mean}}{c_{BW}} = 1 - 2\sum_{n=0}^{\infty}\frac{(-1)^n}{(n+1/2)^2\pi^2}e^{-\frac{(n+1/2)^2\pi^2 D_{py}t_{res}}{d_{zone}^2}}Sin((n+1/2)\pi) \tag{4-9}$$

When the dimensionless time $\frac{D_{py}t_{res}}{d_{zone}^2}$ is 1 or 2 the concentration c_{mean} is already 0.93 and 0.994 c_{BW} respectively. This means that the water leaving the zone is essentially equilibrated with the surface concentration.

For large dimensionless times only one or two terms in the infinite series suffice to obtain accurate results. For short times, however, using the expression for c_{mean} above leads to difficulties because the convergence of the infinite series is very slow and a very large number of terms is needed. However, for short times c_{mean} can be determined by the alternative expression for the concentration profile valid for so short times that the "tip" of the concentration profile not has reached the outer boundary at $y = d_{zone}$.

$$\frac{c}{c_{BW}} = Erfc\sqrt{\frac{D_{py}t_{res}}{4y^2}} \tag{4-10}$$

This is actually the same profile as that used to obtain Equation 3-3.

Integrating this expression from $\frac{D_{py}t_{res}}{d_{zone}^2}$ to $y = d_{zone}$, which for short times is essentially the same as infinity, gives a very simple expression for the mean concentration in d_{zone}.

$$\frac{c_{mean}}{c_{BW}} = \frac{\eta_{mean}}{d_{zone}} = \frac{1.13\sqrt{D_{py}t_{res}}}{d_{zone}} \tag{4-11}$$

For $\frac{D_{py}t_{res}}{d_{zone}^2}$=0.2 the difference between using only the first term in the series and the short time expression is 0.3%. Thus if one uses the short time expression for $\frac{D_{py}t_{res}}{d_{zone}^2}$<0.2 and one term in the series solution for longer times the maximum relative error will be 0.5% at most. 2 terms give at most $3{\cdot}10^{-7}$ relative error in c_{mean}.

We wish to model how much solute, N, will be carried by a stream with flowrate q i.e.

$$N = Q_{eq}c_{BW} = q_{zone}c_{mean} \tag{4-12}$$

then

$$Q_{eq} = q_{zone}\frac{c_{mean}}{c_{BW}} \tag{4-13}$$

Hence, combination with Equation 4-11 shows that

$$Q_{eq} = q_{zone}1.13\frac{\sqrt{D_{py}t_{res}}}{d_{zone}} \tag{4-14}$$

In PA applications q_{zone} is taken from the hydraulic calculation in the fracture network. It can also be estimated from the transmissivity and the hydraulic gradient in the fracture if this is known.

4.4 Estimation of the diffusivities D_{py} and D_{px} in the damaged zone

In the y-direction the tortuosity, i.e. the increase in distance a solute molecule has to travel to move one length unit in the y direction is about τ_y= 10 because of the shape of the rock fragments, /Neretnieks and Andersson 2009/. In the x-direction it is near 1. This is illustrated in Figure 4-3. In the y-direction the solute has to move in sharp zigzag paths whereas in the x-direction the paths are nearly straight.

We then have[1] /Neretnieks 2006b/

$$D_{py} = \frac{D_w}{\tau_y^{\,2}} \tag{4-15}$$

where D_w is the diffusivity in unconfined water. We neglect constrictivity effects along the paths. With a typical value D_w=10^{-9} m^2/s for small solutes in water for the temperature range expected D_{py}= 10^{-11} and D_{px} = 10^{-9} m^2/s.

[1] There is confusion in the literature on how to define the tortuosity. We prefer this notation and meaning.

4.5 An example of mass transfer from the damaged zone to the buffer

To obtain the residence time in the zone, t_{res}, the flowrate q_{zone}, the porosity ε_{zone}, length L_{zone}, width W_{zone}, and thickness, d_{zone}, are needed.

The flowrate in the damaged zone will be about twice that in the fracture intersecting the zone for the same width /Neretnieks 2006b/. In a zone 0.5 m wide the flowrate is the same as in 1 m width of the intersecting fracture.

We show a simple example where we first neglect any mass transfer from the degraded concrete to the buffer. In the next section we analyse the mass transfer from the concrete to the buffer.

For the example below we take the flowrate in a half meter wide W_{zone} of the intersecting fracture to be

$$q_{zone} = T \cdot i \cdot 2W_{zone} \tag{4-16}$$

The length, L_{zone}, in the example is taken to be 10 m, which accounts for the downward leg, and the upward leg in the case where the fracture is located near the top of the deposition hole. The thickness, $d_{zone,}$ is taken to be 0.1 m /Neretnieks 2006b/. Thus only the transfer from the damaged zone to the buffer is accounted for in this case.

The porosity of the zone is not known. However, as the spalling occurs after the deposition hole has been filled with buffer the expansion cannot be larger than the volume of the gap between the rock wall and the buffer. In the example a porosity of ε_{zone}=0.02 is used. The residence time then is

$$t_{res} = \frac{L_{zone} W_{zone} d_{zone} \varepsilon_{zone}}{T \cdot i \cdot 2W_{zone}} = \frac{L_{zone} d_{zone} \varepsilon_{zone}}{T \cdot i \cdot 2} \tag{4-17}$$

The important entity that enters the equations is $\frac{D_{py} t_{res}}{d_{zone}^2}$. It is

$$\frac{D_{py} t_{res}}{d_{zone}^2} = \frac{D_{py} L_z \varepsilon_z}{d_{zone} T \cdot i \cdot 2} \tag{4-18}$$

Equation 4-18 can be used to assess when all the water flowrate q passing through the zone attains the concentration at the buffer surface and when it is only partly equilibrated. This was discussed in the section below Equation 4-9.

With the above data the equivalent flowrate in the damaged zone as a function of transmissivity of the intersecting fracture for gradients 0.001, 0.01 and 0.1 m/m is shown in Figure 4-4. It is unlikely that a locally high gradient will be found in a high transmissivity fracture in a network of fractures with commonly lower transmissivities. The upper right hand part of the figure thus does not show likely values.

It should also be noted that we have used only molecular diffusion to estimate D_{py}. Hydrodynamic dispersion may also add to transverse mixing in the zone and enhance the transport in the y-direction. No information on this effect in the type of rock fragment geometries present in the zone has been found in the literature. Although the flow in the x-direction can be expected to be nearly stratified and strongly channelized because of the shape of the fragments the flow rate between two rock fragments can split when the flow arrives to the next rock fragment and part of it flows on one side of it and the other part flows on the other side of it. If this occurs at many rock fragment tips a solute will spread perpendicularly to the flow direction. This transverse dispersion will enhance spreading of the solute over the zone. The more such mixing locations there are the more efficient will be the transverse dispersion.

Although there are many large rock fragments, which can lead to few mixing locations and strong channelling it cannot be ruled out that transverse dispersion can be considerable and can dominate over molecular diffusion.

As we have not been able to quantify the dispersion we feel it may be prudent to assume that most or all the water in the zone could be equilibrated so that Q_{eq}=q. This would give q=630 litres/yr for T=10^{-7} m^2/s and a gradient of 10%, the highest values used in Figure 4-4.

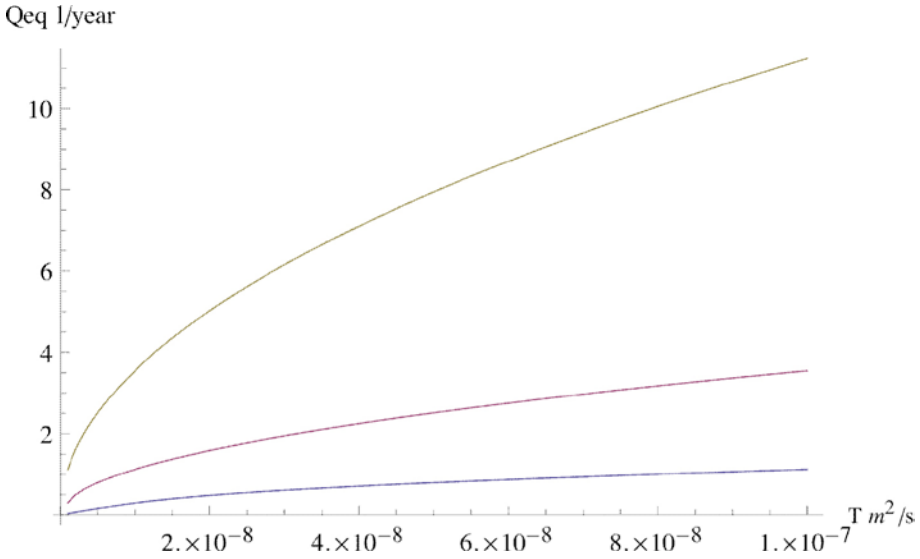

Figure 4-4. *Equivalent flowrate (W_{zone} = 0.5 m, L_{zone}= 10 m, d_{zone} = 0.1 m, ε_{zone}, = 0.02) in the damaged zone as a function of transmissivity of intersecting fracture for gradients 0.001, 0.01 and 0.1 m/m.*

4.6 An example of mass transfer from the degraded concrete to the buffer

It has been suggested that the bottom plate of concrete in each hole could be degraded over very long time by chemical dissolution of the binding minerals in the concrete so that the pore space becomes more permeable to water flow. We explore the consequence in a "what if" scenario assuming that the concrete has a negligible hydraulic resistance and allows water to flow through it.

In the present example the flow enters the damaged zone on one side of the deposition hole moves down and passes through the degraded concrete where after it goes up in the damaged zone on the other side of the deposition hole. The solute has already attained a concentration profile in the passage through the first zone when it enters the degraded concrete. We neglect this and assume that the water is without solute when it enters the concrete. The water spreads out in the circular slab of the bottom zone. The properties of the degraded concrete are very different from those of the damaged zone.

Assuming that the water spreads out uniformly in the concrete and that the residence time for all streamlines is the same, the same equation as used before to assess the mass transfer can be used. The only differences arise from the different thickness of the concrete and the different diffusivity.

The diffusivity is estimated by Archie's law /Archie 1942/, which states that the pore diffusion coefficient is approximately related to the diffusion in the unconfined water by

$$D_p = D_w \varepsilon^{0.6} \tag{4-19}$$

This is used in the example, where the volume of the concrete is taken to be that of a slab with the same diameter as the deposition hole and a thickness of 0.1 m. The porosity $\varepsilon_{concrete}$ = 0.1. This gives a pore diffusion coefficient $D_{p,concrete} = 2.5 \cdot 10^{-10}$ m^2/s. The porosity as well as the diffusion coefficient is thus much larger than in the zone and it can be expected that the mass transfer rate is larger. These data are used in Figure 4-5.

It is seen that the Q_{eq} is much larger than that in the zone shown in Figure 4-4. It would thus seem that the degraded concrete has a strong impact on the mass transfer. However, as shown later in an example, this is only one of the resistances in series that must be considered along this path. The other resistance is that in the buffer. Also for the concrete hydrodynamic dispersion is neglected and also for this case it may be prudent to assume that most or all the water in the zone could be equilibrated so that Q_{eq}=q. This would be much larger than the data shown in Figure 4-5.

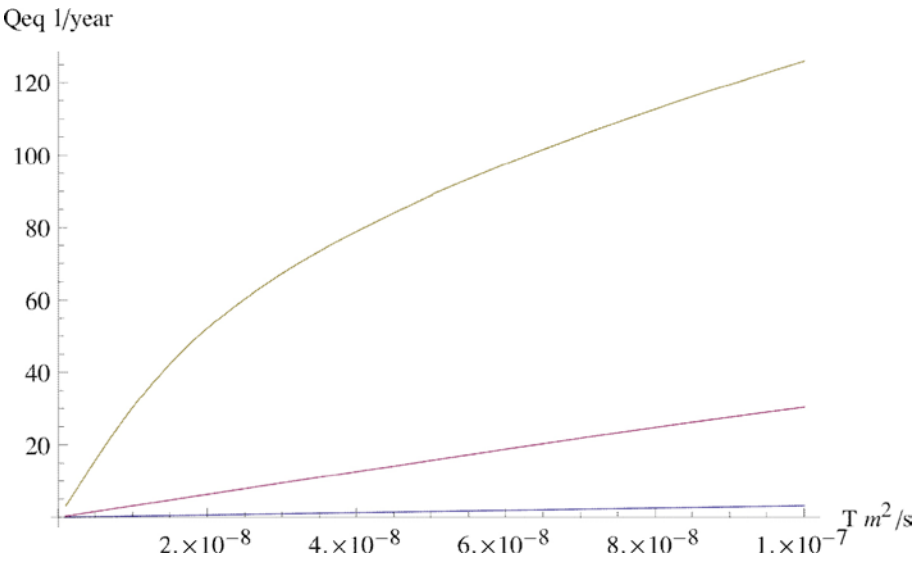

Figure 4-5. *Equivalent flowrate in the degraded concrete as a function of transmissivity of intersecting fracture for gradients 0.001, 0.01 and 0.1 m/m. The geometry of the degraded concrete is taken to be a square L=W with same area as cross section of deposition hole. Concrete is 0.1 m thick.*

5 Mass transfer in buffer and damaged canister

5.1 Large buffer area in contact with a damaged zone and degraded concrete

5.1.1 Mass transfer in buffer in contact with a damaged zone

The transport resistance for a solute in the damaged zone can be expressed as the inverse to the Q_{eq}. A solute will have to pass the buffer also on its way to or from the canister. The resistances are coupled in series and can be added. The inverse of the sum of the resistances will make up the overall equivalent flowrate between canister and water. The largest resistance (smallest Q_{eq}) will dominate the transport.

For transport in the buffer between the damaged zone and the canister surface the transport geometry can be approximated by a slab with the same thickness as the buffer and a cross section area equal to the width of the zone times its length.

The rate of transport through the buffer can be described by Fick's first law

$$N = D_{buffer} A \frac{\Delta c_{buffer}}{d_{buffer}} = D_{buffer} W_{zone} L_{zone} \frac{\Delta c_{buffer}}{d_{buffer}} = Q_{eq,buffer} \Delta c_{buffer} \tag{5-1}$$

Q_{eq} for the buffer then is

$$Q_{eq} = \frac{D_{buffer} W_{zone} L_{zone}}{d_{buffer}} \tag{5-2}$$

With typical values, L_{zone}=10 m, W_{zone}=0.5 m D_{buffer}=10^{-10} m^2/s, d_{buffer}=0.4 m

Q_{eq} is 40 litres/year.

5.1.2 Mass transfer in buffer exposed to a degraded concrete

Similarly one can estimate the mass transfer from the degraded concrete in the bottom of the deposition hole. To exemplify, the cross section area is taken to be that of the deposition hole and the thickness of the buffer d_{buffer}=0.4 m. Using Equation 5-2 applied to the geometry of the concrete, we have

$$Q_{eq} = \frac{D_{buffer} \pi r_h^2}{d_{buffer}} \tag{5-3}$$

Q_{eq} is then 19 litres/year.

5.2 Mass transfer in buffer when a very small buffer area is exposed to solute

When the rock in the deposition hole is not damaged by spalling the solute has to diffuse over the very small area of the fracture as it intersects the buffer. Similarly, a solute that diffuses through a small hole in the canister will expand out into the buffer before it converges to enter the narrow fracture in the rock and the seeping water there.

The solute that emerges from (or converges to) the fracture into the large volume of the buffer will encounter an increasingly larger (or smaller) cross section to diffuse through. The resistance to transport will decrease the farther from the fracture the solute has migrated. Most of the resistance is near the fracture mouth. It has been shown that for typical KBS-3 dimensions the resistance on the average can be described by that equal to that in a thin band at the mouth of the fracture. Taking the thickness of the band equal to the fracture aperture the distance of the band extending into the buffer is 2 to 4 times the fracture aperture depending mainly on the location of the fracture along the deposition hole /Neretnieks 1986/. The diffusion of a solute through such a band can then be obtained as in Section 5.1.1 for the whole buffer to be, if we use the band thickness of 3δ

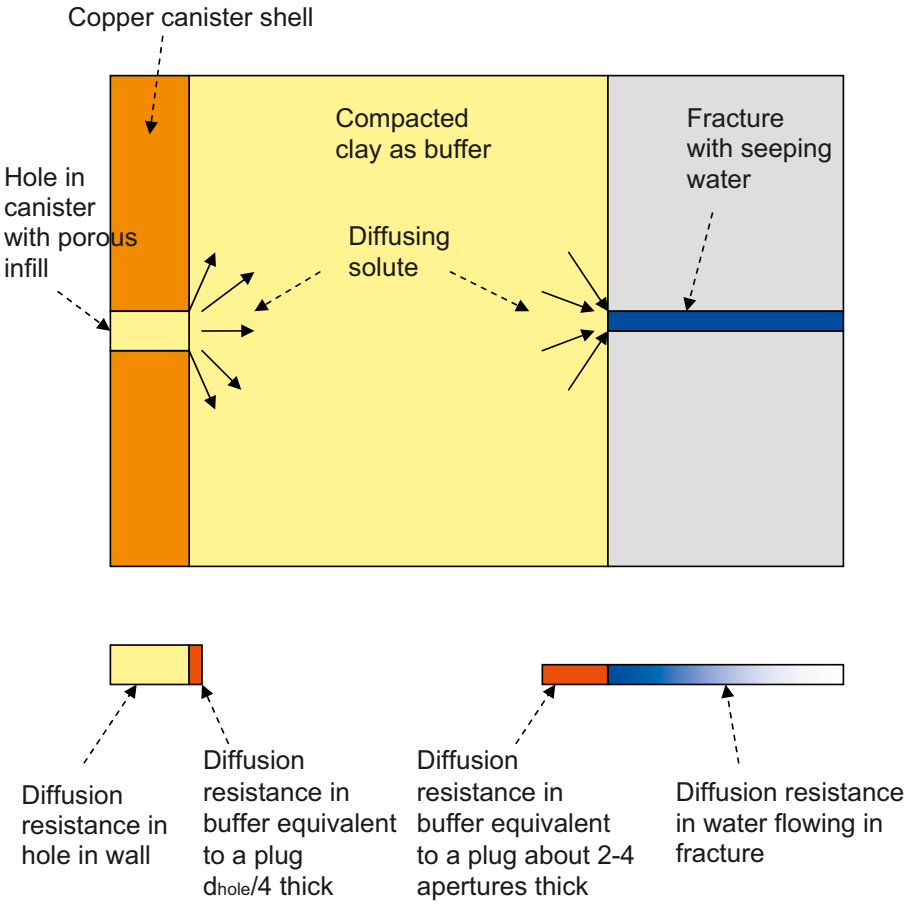

Figure 5-1. *A solute diffuses from the interior of the canister through a small hole in the canister, out into the buffer before it again converges to diffuse into the narrow fracture and the seeping water.*

$$N = D_{buffer}\frac{2\pi r_h \delta}{Cos\alpha}\frac{\Delta c_{buffer}}{3\delta} = D_{buffer}\frac{2\pi r_h}{3\,Cos\alpha}\Delta c_{buffer} = Q_{eq}\Delta c_{buffer} \quad (5\text{-}4)$$

Q_{eq} then is

$$Q_{eq} = D_{buffer}\frac{2\pi r_{hole}}{3\,Cos\alpha} \quad (5\text{-}5)$$

Δc_{buffer} is the concentration difference between the mouth of the fracture and that at the canister surface.

With typical values for the buffer r_h = 0.875 m, D_{buffer}=10^{-10} m^2/s and taking the intersecting angle $\alpha = \pi/4$

Q_{eq} = 8.2 litres/year

5.3 Mass transfer through a hole in the canister

Q_{eq} for the straight hole in the canister is

$$Q_{eq} = D_{corr}\frac{\pi r_d^2}{d_{Cu}} \quad (5\text{-}6)$$

D_{corr} is the diffusion coefficient in the corrosion products in the hole in the canister. The other dimensions are explained in Figure 5-2.

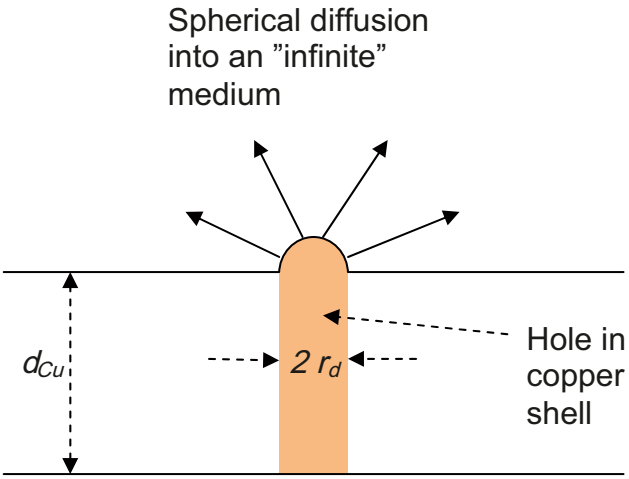

Figure 5-2. *A solute diffuses through a small cylindrical hole in the copper canister shell and out into an "infinitely" large buffer. At the mouth of the hole a half sphere is the boundary between corrosion products and buffer.*

To exemplify, with D_{corr}= 10^{-10} m^2/s, r_d = 1 mm and d_{Cu}=50 mm

Q_{eq} = $2 \cdot 10^{-4}$ litres/year

A 10 mm radius hole still gives only a

Q_{eq} = 0.02 litres/year

The transport capacity through the hole is thus very small compared to the all other Q_{eq}'s discussed earlier.

5.4 Mass transfer from a small hole in the canister into a large buffer volume

The transport capacity from the mouth of the hole through the buffer can be approximately obtained when the extent of the buffer is much larger than the dimensions of the hole as follows. As shown in Figure 5-2, the interface between the corrosion products in the copper and the buffer is assumed to form a half-sphere where there is a concentration c_o at the spheres surface.

The buffer can be approximated to be "infinite" and have a concentration equal to c_∞ far away. The concentration on the half-sphere is c_0.

The rate of transport N through a half sphere with radius r is given by

$$N = -D_{buffer} 2\pi r^2 \frac{dc}{dr} \tag{5-7}$$

As N is constant Equation 5-7 can be integrated to obtain the concentration profile extending from the mouth of the hole to distance r.

$$c(r) - c_o = \frac{N}{2\pi D_{buffer}} \left(\frac{1}{r} - \frac{1}{r_d}\right) \tag{5-8}$$

When $r >> r_d$

$$\Delta c = c_o - c_\infty = \frac{N}{2\pi D_{buffer}} \frac{1}{r_d} \tag{5-9}$$

and

$$Q_{eq} = 2\pi r_d D_{buffer} = \frac{\pi r_d^2 D_{buffer}}{r_d/2} = \frac{A_{plug} D_{buffer}}{d_{plug}} \quad (5\text{-}10)$$

The rightmost expression in Equation 5-10 shows that Q_{eq} can be interpreted as the transport capacity through a cylindrical plug with radius r_d and thickness $r_d/2$. This was illustrated in Figure 5-2.

To exemplify, with D_{corr}= 10^{-10} m^2/s, r_d = 1 mm

Q_{eq} =0.02 litres/year

A hole diameter r_d = 10 mm gives

Q_{eq}=0.2 litres/year.

5.5 Impact of a fractured cemented buffer

Should the buffer by some reason be cemented and become brittle it might develop cracks. We have explored the consequences of the presence of a crack that extends all the way through the cemented buffer and which connects to the fracture in the rock with the seeping water. If the crack in the buffer has a larger transmissivity than that in the rock the water flowrate in the rock fracture will be somewhat increased. The major impact is, however, that the seeping water now comes in direct contact with the copper canister and can deliver any corrosive agent directly to the surface of the copper canister. In the presence of an undamaged buffer the corrosive agent would diffuse out into the buffer up as well as downward in the deposition hole and spread out over a large surface area of the canister. With a crack in the buffer the corrosive agent will react in the very narrow region where the crack is in contact with the canister. Corrosion would be very localised. These conditions are described and modelled in /Neretnieks 2006a/ where also sample calculations are given.

The corrosion is expected to spread out radially into the canister from the intersection with the fracture. This is shown in Figure 5-3.

Figure 5-3 shows the basic model structure used to quantify the size of the corrosion area on the copper canister.

Water that flows in the fracture carries sulphide or sulphate that could be reduced to sulphide by microbially mediated reactions at the canister surface. The copper is corroded in a thin slit where the fracture intersects the canister. A mass balance can be formulated by assuming that the canister at the intersection corrodes as a half cylinder into the copper. All the sulphide carried by the Q_{eqFB} in the fractured buffer is transformed to Cu_2S and remains in the location where the copper corroded. When the half cylinder has attained a radius equal to the thickness of the copper canister wall it is breached. We wish to calculate the time for this to happen. The copper volume V_{Cu} in the half cylinder which extends all around the canister is that of a half cylinder which is $2\pi r_{can}$ long and with a cross section $\pi \cdot Cu_{Thickness}^2/2$. In a first approximation the time to breach the canister is then given by Equation 5-11.

$$t_{breach} = \frac{V_{Cu}}{Q_{eqFB} c_{S^{2-}}} \frac{\rho_{Cu}}{2M_{Cu}} \quad (5\text{-}11)$$

The first approximation can be improved by also accounting for the diffusion resistance of the copper corrosion products. The sulphide from the flowing water has to diffuse through the corrosion products in the half cylinder to reach the remaining intact copper. The diffusion resistance in this half cylinder is added to that in the flowing water. The equivalent flowrate accounting also for the resistance in the corrosion products Q_{eq}^{tot} is obtained by solving the diffusion equation for the half cylinder along all its length $2\pi r_{can,}$ see /Bird et al. 2002 p 305/. It is

$$Q_{eq}^{tot} = \frac{1}{\frac{1}{Q_{eqDZ}} + \frac{Ln(r/r_i)}{2\pi r_{can} \pi D_{Cu2S}}} \quad (5\text{-}12)$$

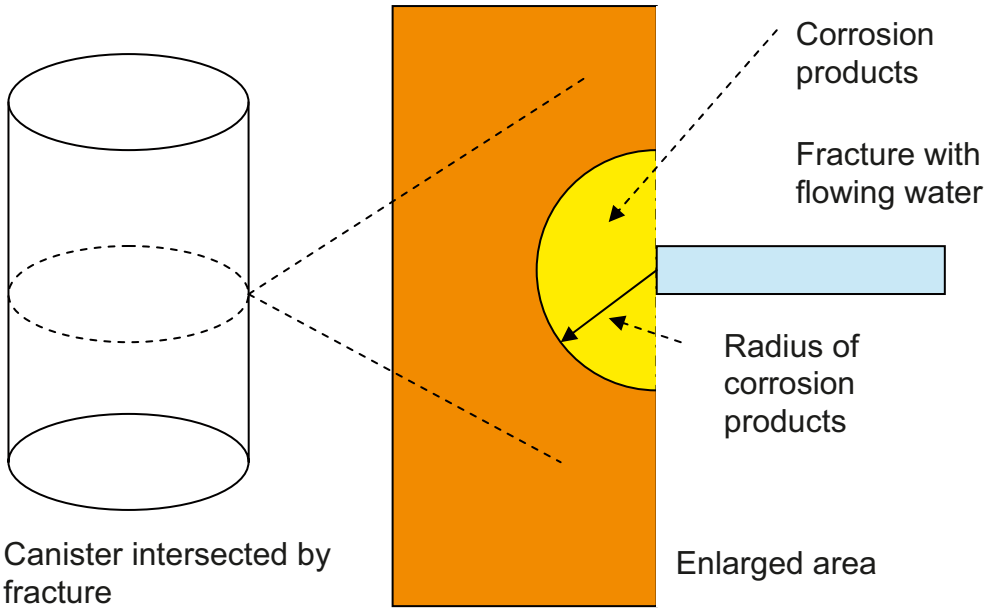

Figure 5-3. *Canister intersected by a fracture in the cemented buffer. Corrosion in a half cylindrical region all around the canister circumference.*

here r_i is taken to be half the aperture of the crack in the buffer. The radius of the corroded half cylinder region changes as the corrosion progresses. The mean of the combined equivalent flowrate is therefore obtained by integrating the above Equation 5-12 from r=r_i to r=copper thickness =r_y.

$$Mean Q_{eq}^{tot} = \frac{1}{r_y - r_i} \int_{r_i}^{r_y} \frac{dr}{\frac{1}{Q_{eqDZ}} + \frac{Ln(r/r_i)}{2\pi r_{can} \pi D_{Cu2S}}} \tag{5-13}$$

Evaluating this expression one finds that the influence of the resistance of the corrosion products is small. It adds less than 10% to the corrosion time.

6 Overall Q_{eq} from water to canister surface

The examples below serve to illustrate how the resistances can be added to obtain the overall equivalent flowrates. For simplicity we only exemplify the transport from the water to the canister surface as for a corrosive agent. For escaping nuclides the two additional resistances in the hole in the copper and from the hole will be added.

6.1 No damaged zone or degraded concrete

In this case there are two resistances in series; that in the seeping water in the fracture and that in the buffer. The latter is modelled by the diffusion through the thin buffer plug. In the example it is Q_{eqB}=8 litres/year (see Section 5.2). The largest value for the seeping water is Q_{eqW}= 4 litres/year, as shown in Figure 3-3 Equation 2-1 then gives

$Q_{eq}^{overall}$ = 2.7 litres/year.

With lower flowrates in the fracture the resistance will be dominated by the transport in the water and $Q_{eq}^{overall}$ can become very low.

6.2 Presence of damaged zone and degraded concrete

When there are damaged zones and degraded concrete allowing the water to pass them in series this can be modelled as two parallel paths for solute exchange between canister and water as discussed previously. In each of these paths there are resistances (i.e. the inverse of the equivalent flow rates) in series that can be added to obtain the overall resistance.

In the example below the Q_{eq} in each path is first determined by adding the resistances and then the overall Q_{eq} for both paths are added. The Q_{eq} data are taken from the previous examples.

For the path through the damaged zone and then the buffer the Q_{eq} for the highest transmissivity and gradient is used. This is Q_{eqW}=10 litres/year (Figure 4-4). For the buffer Q_{eqB}=40 litres/year (Section 5.1.1). Then with Equation 2-1 the overall Q_{eq}=8 litres/year.

Similarly for the concrete path, Q_{eqW}=110 litres/year (Figure 4-5), Q_{eqB}=19 litres/year (Section 5.1.2), resulting in Q_{eq}=16 litres/year.

Together this makes $Q_{eq}^{overall}$ =24 litres/year.

6.3 Total loss of buffer

All the above resistances to mass transfer disappear if the buffer is lost in the very pessimistic scenario of the performance assessment. Then the deposition hole acts as a sink and draws in water from the fracture(s) intersecting the hole. The flowrate through the hole can be estimated by Equation 4-16 using the cross section of the deposition hole instead of the width of the damaged zone. The water in the now empty hole must be assumed to mix by convective currents in addition to diffusion so that the water would be fully depleted of e.g. a corrosive agent. Q_{eq} will then be equal to the total flowrate q.

$$q_{nobuffer} = T \cdot i \cdot 2 \cdot \frac{2r_h}{Cos\alpha} \tag{6-1}$$

With r_h=0.875 m, α = π/4, T= 10^{-7} m^2/s and i=0.1

$Q_{eq}^{overall}$ $q_{nobuffer}$ = 1,560 litres/year

The specific equations for this case are shown in the Appendix.

6.4 Fractured buffer

An example aiming to illustrate the rate of corrosion of the copper canister when the buffer is cemented and a crack has developed through the buffer is given below.

For a transmissivity of 10^{-8} m^2/s and a gradient 0.01, Q_{eq} is a fraction of a litre per year as can be seen in Figure 3-3. With this and the data in Table 6-1 the time to breach the 50 mm thick canister wall is tens of million years. The diffusivity in the corrosion products must be at least one order of magnitude lower to have a serious influence. The value used here would be applicable to a corrosion product with porosity on the order of 10–20%. As there are no data for this entity it cannot be relied on to have an important effect.

The sulphide concentration in the example was chosen to be 1 mg/litre. Natural waters have lower concentrations, which would lead to longer corrosion times. Should there be sulphide formation by microbially mediated sulphate reduction it is conceivable that a higher value for sulphide concentration could be appropriate. Then the time should be proportioned accordingly.

Table 6-1. Data for the corrosion example.

Entity	Meaning	Value
r_i	Half fracture aperture	0.5 mm
r_y	Copper thickness	50 mm
r_{can}	Radius of canister	0.525 m
D_{Cu2S}	Diffusivity in corrosion product (Rough estimate)	10^{-10} m^2/s
M_{Cu}	Molecular weight of corrosion product	63.54 g/mol
ρ_{Cu}	Density of corrosion product	8,920 kg/m^3
c_{S2-}	Sulphide concentration in water	$3 \cdot 10^{-5}$ M (1 mg/litre)

7 Discussion of concepts and assumptions

7.1 Conceptual model

The conceptual model is very simple. Water seeps in a fracture that intersects the canister deposition hole. Solute(s) migrate by molecular diffusion between the bulk of the water and the interface with the buffer and from there through the buffer to the canister surface.

Molecular diffusion is a well known and understood process and data on diffusivities are available. It is common practice in such situations to describe these systems as a number of resistances in series. Each resistance to mass transfer can then be added similarly to how resistances in an electrical circuit are added. The driving force for the solute migration (i.e. concentration difference) is then analogous to the voltage difference in the electrical circuit.

The resistance to mass transfer is proportional to the length of the path and inversely proportional to the cross section area. This is also in full analogy with the electrical resistance.

For the seeping water in the fracture advective flow helps transport the solute to/from the buffer in addition to diffusion.

The residence time of the water at the buffer/water interface, and the contact area will determine the rate of mass transfer between water and buffer.

The sum of the resistances determines the overall resistance to mass transfer and sets the overall rate of solute transport.

When there are parallel migration paths in addition to those in series such networks of resistances are handled in the same way as electrical networks. In the present application mostly resistances in series have been considered.

The concept of an equivalent flow rate was introduced as a means of illustrating how much solute, e.g. a corrosive agent could be transported to a canister from water containing a known concentration of the solute. Alternatively it can be used to assess the rate of nuclide escape from the canister.

7.1.1 Diffusion in a porous medium

Fick's first law is used to describe the rate of steady state transport by molecular diffusion in a porous medium. For a constant cross section area it states that the rate of transport is proportional to the concentration difference and the cross section area and inversely proportional to the thickness of the medium. It is readily extended to complex two and three-dimensional geometries.

Analytical methods can often be used to obtain mathematical solutions for solute transport in simple geometries. For complex geometries numerical methods are used. In some cases approximate analytical methods are useful because, although simplifying assumptions are used that introduce some deviation from the "exact" solution the solution is accurate enough for the purpose and is transparent and simple. Comparisons with numerical solutions show good agreement, /Kelly and Cliffe 2006/.

Fick's second law can be seen as an extension of the Fick's first law and allows the concentration to change in time and space. It essentially is a mass balance of the solute stating that what diffuses into a small element and does not diffuse out during the same time period will accumulate, increasing (or decreasing) the concentration at that location.

The Q-equivalent approach is, as we discussed above, closely related to Fick's first law. The conditions when this approach is inadequate and a solution of Fick's second law is required are to be discussed in Section 7.2.1.

7.1.2 Flow and diffusion

In seeping water advection (flow) will transport the solute in addition to molecular diffusion. Similarly to what was done in Fick's second law a mass balance can be made for the solute that both flows and diffuses in and out of a small element.

This principle was applied to the seeping water in the fracture as the water passes the vicinity of the buffer. A large number of elements must be considered simultaneously. This is done in numerical methods. Analytical methods can be used to solve the problem for simple geometries where the elements are made vanishingly small. Analytical methods were used to obtain the solutions for flow in fractures and in the damaged zone. These solutions have been compared with solutions obtained by numerical methods. The agreement is excellent /Kelly and Cliffe 2006/.

The above simplified description of the flow and transport has been extensively used in much more complex situation in the so called Boundary Layer Theory. Also the descriptions of mass transfer resistances and mass transfer rates are extensively used in chemical engineering in the so called Film Resistance notion. There is vast experimental evidence supporting these theories.

7.2 Revisiting assumptions

The simple models presented in this report are based on a number of assumptions. The most important assumptions, how reasonable they are and their impact on the modelling results are discussed in this section.

The assumptions are

- Steady state
- Laminar flow and mixing by diffusion
- The solute concentration at the buffer/water interface is the same everywhere at the interface
- The fractures are narrow enough that the viscous boundary layer can be neglected when calculating solute advection along the buffer/rock interface
- Pe > 4.

7.2.1 Steady state assumption

It was assumed that the water flowrate in the fracture is constant over time. This is partly motivated by use of flow rate information taken from fracture network hydraulic modelling where flowrate is constant over a longer period. It is also a reasonable assumption from the point of view of the time it takes for a steady state concentration profile to build up compared to the time it takes for the flowrate or the concentration to change. The time to establish a steady state can be determined by solving the equations for an instationary case. However, we use a simpler but more illustrative approach. The characteristic time for a concentration to attain steady state in the seeping water in the fracture after a change in flowrate or change in concentration at the boundaries is assessed from the time it takes for the profile to reach the outer boundary for the case considered. For example for the damaged zone it could be taken as the thickness of the zone, i.e. 0.1 m. For the flow around the buffer in the fracture a characteristic time can be taken as the time to practically saturate the water at a distance on the order of the radius of the deposition hole at most. This distance is approximately that which sets the validity of the model with Pe>4.

Practical equilibrium will be attained at time t_{ss} when

$$\frac{D_{py} t_{ss}}{d_{zone}^2} = 1 \qquad (7\text{-}1)$$

in the zone and

$$\frac{D_w t_{ss}}{r_h^2} = 1 \qquad (7\text{-}2)$$

for the seeping water at most when the penetration depth is comparable to the radius, which is when the validity criterion Pe>4 is attained. In both cases $t_{ss} \cong 30$ years

Thus if flowrates or concentrations were to change more rapidly than in 30 years the steady state assumption would be violated. This is not expected.

For the concentration build-up in the buffer the same approach can be used but then retardation due to sorption and nuclide decay must be accounted for.

In this case

$$\frac{D_{buffer}}{R_{Nu}} \frac{t_{ss}}{d_{buffer}^2} = 1 \qquad (7\text{-}3)$$

and

$$t_{ss} = \frac{d_{buffer}^2}{D_{buffer}} R_{Nu} \cong 50 R_{Nu} \quad \text{(in units of years)} \qquad (7\text{-}4)$$

This gives approximately t_{ss}=50 R_{Nu} years for a buffer thickness of 0.4 m.

Retardation factors R_{Nu} can be much larger than 1 for many sorbing nuclides. Then the steady state approximation may be violated. Similarly nuclides with half-lives shorter than t_{ss} will also violate the assumption. When the assumption is violated full transient calculations must be made. The analytical solutions for the rim and the plugs can then be embedded in the numerical schemes. In this way considerable saving in computational effort can be made without loss of accuracy, /Kelly and Cliffe 2006/.

7.2.2 Assumption that the flow is laminar and that mixing occurs by diffusion

The assumption that the flow is laminar in the fractures and in the damaged zone is the basis for the use of molecular diffusion as the sole mechanisms of solute mixing between streamlines.

Flow in even rough walled conduits is safely laminar if the Reynolds's number Re, is smaller than 1.

$$\mathrm{Re} = \frac{u \delta \rho_w}{\eta_w} \qquad (7\text{-}5)$$

Where ρ_w =1,000 kg/m^3 is the density of water, η_w = 0.001 Pa s is the viscosity and u is the water velocity $u = Ti/\delta$.

Even for the highest reasonable transmissivity and gradient, T=10^{-7} m^2/s and i=0.1 m/m, a marginal value of Re ≈ 0.01 would be the result. The fact that Re< 0.1 ensures laminar flow.

Similarly the flow in the damaged zone will be laminar as the water velocity is lower in the multitude of fractures in the zone. This will also be true for degraded concrete.

7.2.3 Assumption that solute has the same concentration at the interface between water and buffer

The assumption that solute has the same concentration at the interface between water and buffer is useful to avoid the need to solve the flow and transport equation in two dimensions in the fracture at the same time as a three dimensional treatment of the solute diffusion in the buffer would be needed.

In reality the mass transfer rate is higher on the upstream side of the deposition hole than on the downstream side. This in turn influences the diffusion in the buffer in a complex way.

The assumption that the concentration at the interface is constant introduces an error that depends on buffer geometry and relative diffusivities in water and buffer. This error is quite certainly less than what is due to the uncertainties in fracture aperture, fracture aperture variations flowrates etc. It has therefore not been deemed necessary to make a more detailed analysis of this assumption /NAGRA, 1994/.

7.2.4 Other assumptions deemed to be of minor importance

The assumption that Darcy law is valid locally has been tested repeatedly in several studies and it has been found that “exact” numerical solutions of the flow and transport equations in variable aperture fractures agree reasonably well with the simplified case.

Channelling effects are deemed to be sufficiently well handled by the studies of variable aperture fractures considering the poor knowledge of aperture variations in real fractures.

The assumption that no buffer has expanded out in the fractures is conservative as such event would strongly decrease the overall mass transfer due to the presence of an additional barrier.

It is assumed that diffusion through the rock matrix to and from the buffer is negligible compared to the other transport paths. This has been previously tested by scoping calculations and found to be true /Nilsson et al. 1991/.

The flow velocity in the damaged zones and in the concrete is assumed to be constant i.e. there are no channels with higher flow. In reality very strong channelling is expected in both regions. Then much or even most of the water will have a considerably lower residence time than the mean and mass transfer will be lower in the damaged zone as well as in the concrete. The plug flow model is conservative.

8 Discussion of examples

8.1 Summary of data used in the examples

In Table 8-1, we summarize the data used in the calculations in the report. These data are all within the ranges expected for a KBS-3 repository.

8.2 Comments on the examples

8.2.1 Fracture flow

The example of Q_{eq} for flow in fractures shown in Figure 3-3 is not realistic for the combination of high transmissivity and high gradient because in a fracture network with stochastically variable transmissivities a high transmissivity fracture will most likely be connected to low transmissivity fractures. These will limit the flowrate through the high transmissivity fracture.

One and the same aperture is used in the example for high transmissivity and low transmissivity fractures. Probably the high transmissivity fractures will have larger apertures and somewhat counteract the effect of the lower flowrates.

8.2.2 Damaged zone and degraded concrete

In the example the bottom of the deposition hole is permeable and connects the two damaged sides of the deposition hole. This permits a larger flowrate and larger contact area between water and buffer than if the bottom was tight.

The porosity of the damaged zone is poorly known and will depend much on if the presence of the buffer has restrained expansion of the zone. The hydraulic conductivity was assumed to be in practice infinitely large permitting much water to be drawn in from the intersecting fracture. Some buffer can be expected to expand into the larger fractures and decrease the flowrate as well as the contact area between seeping water and buffer.

Table 8-1. Summary of main data for the examples.

Entity	Meaning	Value
r_h	Radius of deposition hole	0.875 m
ε_{zone}	Porosity of damaged zone	0.02
L_{zone}	Length of damaged zone	10 m
W_{zone}	Width of damaged zone	0.5 m
d_{zone}	Thickness of damaged zone	0.1 m
d_{buffer}	Thickness of buffer	0.4 m
$d_{concrete}$	Thickness of concrete	0.1 m
$\varepsilon_{concrete}$	Porosity of degraded concrete	0.1
D_w	Diffusivity in water	10^{-9} m^2/s
D_{buffer}	Diffusivity in buffer	10^{-10} m^2/s
D_{corr}	Diffusivity in copper corrosion products	10^{-10} m^2/s
τ_y	Tortuosity in radial direction in damaged zone	10
δ	Fracture aperture	0.1 mm
T	Transmissivity of fracture	10^{-9} to 10^{-7} m^2/s
i	Hydraulic gradient	0.001, 0.01, 0.1

In the examples the damaged zone and the degraded concrete were treated independently although it is the same water that exchanges solute with the buffer. Unless all the water is already equilibrated when it has passed the downward leg in the zone the water will also exchange solute as it passes the concrete and the upward leg. The Q_{eq}'s for paths zone and concrete are not additive. Furthermore, the transport path from water in the zone and then through the buffer to the canister is parallel to that from the water in the degraded concrete and buffer below the canister. This situation cannot be *correctly* described by the simplified Q_{eq} concept. However, treating the two parallel paths, i.e. from zone to canister and from concrete to canister as if they were entirely independent and adding the two *overall* Q_{eq}'s in each path will not introduce undue errors The maximum error will be on the order the smallest of the flowrates and will be conservative as it exaggerates to the rate of transport.

8.2.3 Buffer and canister wall

The presence of a damaged zone allows the solute transport through the buffer to be essentially linear and to utilize a large cross section area for transport through the buffer. This results in a low transport resistance.

Without the damaged zone the narrow fracture aperture will force the solute to expand from or converge to the narrow fracture, which markedly increases the resistance.

Similarly a nuclide escaping from the interior of the canister will emerge from a narrow hole. This migration path has a very strong resistance as long as the hole is small in comparison to the buffer thickness. The plug model gives a good approximation when the hole diameter is less than 10 percent of the buffer thickness as can be seen in the derivation of Equation 5-9 from Equation 5-8.

The by far largest resistance to nuclide escape is through the narrow (mm size) hole in the canister wall.

8.3 Summary of examples

Table 8-2. Summary results from the examples.

Individual Q_{eq}'s	Section	Q_{eq} litres/year
Fracture with seeping water	3.4 (Figure 3-3)	<0.01–4
Variable aperture fracture	3.5 (Figure 3-5)	Variation is plus/minus 80%
Damaged rock zone with seeping water	4.5 (Figure 4-4)	<0.01–10
Degraded concrete with seeping water	4.6 (Figure 4-5)	<0.1–120
Buffer when there is rock damage	5.1.1	40
Buffer above degraded concrete	5.1.2	19
Rim at fracture mouth	5.2	8
Mouth of canister hole for 1 mm radius	5.3	0.02
Hole in canister for 1 mm radius	5.3	0.0002
Overall Q_{eq}'s		
Damaged rock and concrete adding both paths and resistances in them	6.2	24
Total lost of buffer	6.3	1,560

9 Overall discussion and conclusions

Solute exchange between the canister and seeping water in the rock is governed by molecular diffusion in a complex geometrical setting. Fractures with seeping water can intersect the deposition hole at any angle and at any location. The rock may have been exposed to so high stresses that damaged zones may have formed along the deposition hole and the concrete at the bottom of the hole may have been degraded giving it a high hydraulic transmissivity. The damaged zone is also expected to have a high hydraulic conductivity, which will facilitate for the water seeping in the fractures intersecting the hole to flow there. The hydraulic and other properties of the concrete and zones are poorly known. It is reasonable to assume that they do not act as barriers to flow and that solutes can migrate by molecular diffusion in them.

Although it is feasible to fairly accurately assess the solute migration paths and rates by numerical methods for a given situation, should good data be available, this is a fairly demanding numerical task. Further one would need to do a large number of simulations for different geometries, water flowrates in fractures etc.

In this report we make some simplifying assumptions that make it possible to derive some very simple equations that describe the different mass transfer resistances in the system. As in most cases the resistances are coupled in series they can be added to give the mass transfer resistance for a given migration path and scenario.

The mass transfer rate can then be visualised in a simple way by the inverse of the resistance which we denote Q_{eq}. For example for a corrosive agent this is an equivalent flowrate that is depleted of all its concentration of corrosive agent. It can also be used to visualise how much water would be contaminated by a nuclide with its solubility concentration. It is a convenient way of comparing the transport capacity of different flowpaths and different scenarios.

All the underlying mechanisms described by the models for the different resistances are based on fundamental laws of physics and chemistry. The conceptual basis for adding transport resistances and for making the simplifying assumptions have been used in chemical engineering and other disciplines for a very long time and have been validated by numerous experiments.

The uncertainties in the simplified models are deemed to be small compared to the uncertainties in especially the flow rates in the fractures, the properties of the damaged zones and concrete and for the different geometrical possibilities.

10 Notation

A	Cross section for diffusion	m^2
c	Concentration	mol/m^3
c_{buffer}	Concentration in the buffer	mol/m^3
c_{BW}	Concentration at buffer/water interface	mol/m^3
c_o	Concentration inside canister or at canister surface	mol/m^3
c_w	Concentration in seeping water	mol/m^3
c_∞	Concentration far away from the surface	mol/m^3
C_{eq}	Constant in Equation 3-9	–
d_{buffer}	Thickness of buffer	m
d_{Cu}	Thickness of copper shell	m
d_{zone}	Thickness of damaged zone	m
D_{buffer}	Effective diffusion coefficient in buffer	m^2/s
D_{corr}	Effective diffusion coefficient in copper corrosion products	m^2/s
D_p	Pore diffusion coefficient	m^2/s
D_{px}	Pore diffusivity in the x-direction	m^2/s
D_{py}	Pore diffusivity in the y-direction	m^2/s
D_w	Diffusion coefficient in water	m^2/s
f_s	Shape factor	–
i	Hydraulic gradient	m/m
K	Hydraulic conductivity	m/s
l	Length in direction parallel to flow,	m
l_c	Correlation length	m
L	Length in flow direction	m
L_{zone}	Length of damaged zone	m
N	Flowrate of solute	mol/s
Pe	Peclet number	–
q	Flowrate	m^3/s
q_{zone}	Flowrate in zone	m^3/s
Q_{eq}	Equivalent flowrate	m^3/s
Q_{eqW}	Equivalent flowrate at the water/buffer interface	m^3/s
Q_{eqFB}	Equivalent flowrate for fractured buffer	m^3/s
Q_{eqDZ}	Equivalent flowrate for damaged zone	m^3/s
r_{can}	Radius of canister	m
r_d	Radius of hole through copper canister	m
r_h	Radius of deposition hole	m
r_s	Equivalent radius of deposition hole	m
R	Resistance to mass transfer	s/m^3
Re	Reynolds number	–
R_{Nu}	Retardation factor in buffer	–
S_i	Area of the intersection with deposition hole	m^2
t	Time	s

t_{breach}	Time to breach canister	s
t_{res}	Water residence time	s
t_{ss}	Time for a concentration to attain steady state in the seeping water	s
T	Transmissivity of fracture in rock	m^2/s
u	Velocity	m/s
V_{zone}	Volume of eroded buffer	m^3
w	Width in direction normal to flow	m
W_{zone}	Width of damaged zone	m
W	Width perpendicular to flow	m
x	Space coordinate	m
y	Space coordinate	m
X	Dimensionless space coordinate	–
Y	Dimensionless space coordinate	–

α	Angle between fracture plane and the horizontal	rad
δ	Fracture aperture	m
ε	Porosity	–
ε_{zone}	Porosity of zone	–
μ	Mean aperture	m
η_{mean}	Mean penetration depth	m
η_w	Viscosity of water	Pas
ρ_{Cu}	Density of copper	kg/m^3
ρ_w	Density of water	kg/m^3
σ	Standard deviation of apertures	m
τ	Tortuosity	–

11 References

Andersson J C, 2007. Äspö Pillar Stability Experiment, Rock mass response to coupled mechanical thermal loading, SKB TR-07-01, Svensk Kärnbränslehantering AB.

Archie GE, 1942. The electrical resistivity log as an aid in determining some reservoir characteristics, Petroleum Transactions of AIME 146: p 54–62.

Bird R B, Stewart W E, Lightfoot E N, 2002. Transport phenomena, 2nd ed. Wiley.

Chambré P L, Pigford T H, Fujita A, Kanki T, Kobayashi A, Lung H, Ting D, Sato Y, Zavoshy S J, 1982. Analytical performance models for geologic repositories. LBL-UCB-NE-4017, UC70. Earth Sciences Division, Lawrence Berkeley Laboratory and Department of Nuclear Engineering, University of California, Berkeley, California, 94720 USA. Report prepared for the U.S. Department of Energy.

Comsol Multiphysiscs™, 2005. Comsol AB.

Keller A A, 1997. High resolution CAT imaging of fractures in consolidated materials, International Journal Rock Mech. Min. Sci. 34, 3/4, p 3385.

Kelly M, Cliffe K A, 2006. Validity document for COMP23, SKB R-06-76, Svensk Kärnbränslehantering AB.

Liu L, Neretnieks I, 2004. Fluid flow and solute transport through a fracture intersecting a canister – Analytical solutions for the parallel plate model, Mat. Res. Soc. Symp. Proc. 807.

Liu, L, Neretnieks I, 2005a. Analysis of fluid flow and solute transport in a fracture intersecting a canister with variable aperture fractures and arbitrary intersection angles, Nuclear Technology, 150, p 132–144.

Liu L, Neretnieks I, 2005b. Analysis of fluid flow and solute transport through a single fracture with variable apertures intersecting a canister: Comparison between fractal and Gaussian fractures, Material Research Society 05.

NAGRA, 1994. Technical Report 93-22 Kristallin-I Safety Assessment Report. NAGRA NTB 93-22.

Neretnieks I, 1979. Transport mechanisms and rates of transport of nuclides in the geosphere as related to the Swedish KBS concept. Proceedings, International Atomic Energy Agency IAEA – SM – 243/108, p 315–339, July 2–6, 1979.

Neretnieks I, 1986. Stationary transport of dissolved species in the backfill surrounding a waste canister in fissured rock – A simple analytical solution. Nuclear Technology 72, p 194–200.

Neretnieks I, 2006a. Flow and transport through a damaged buffer – exploration of the impact of a cemented and an eroded buffer, SKB TR-06-33, Svensk Kärnbränslehantering AB.

Neretnieks I, 2006b. Flow and solute transport in a zone damaged due to spalling, SKB R-06-91, Svensk Kärnbränslehantering AB.

Neretnieks I, Andersson J C, 2009. Characterisation of spalling fragments to obtain data for flow and transport in damaged zones. Paper presented at “Sinorock 2009” Congress 19–22 May 2009, Hongkong, Proceedings.

Nilsson L, Moreno L, Neretnieks I, 1991. A resistance network model for radionuclide transport in the near field surrounding a repository for Nuclear waste, SKB TR 91-30, Svensk Kärnbränslehantering AB.

Process report, 2006. Buffer and backfill process report for the safety assessment SR-Can, SKB TR-06-18, Svensk Kärnbränslehantering AB.

Q_{eq} for flow in eroded buffer

The water that flows in the eroded volume around the canister will deposit a solute migrating to the canister or take up a solute from the canister by molecular diffusion. The longer the water is in contact with the canister the more solute can be transferred. We use a simplified model to describe the system and to quantify the equivalent flowrate. The figure below shows how the system is conceptualized and simplified. The canister and rock curvature are straightened out and the flow is now linear. Symmetry is assumed in the z-direction.

The solute concentration over time and in space in the water is described by the partial differential equation.

$$\frac{\partial c}{\partial t} + u\frac{\partial c}{\partial x} = D_w\left(\frac{\partial^2 c}{\partial x^2} + \frac{\partial^2 c}{\partial y^2}\right)$$

This equation can be simplified as we only consider a stationary case when the concentration does not change over time but only in space. Then $\frac{\partial c}{\partial t}$=0 and

$$\frac{\partial c}{\partial t_{res}} = D_w\left(\frac{\partial^2 c}{\partial x^2} + \frac{\partial^2 c}{\partial y^2}\right)$$

Where t_{res} is x/u. Thus only the residence time of the water need be accounted for. A further simplification is made by neglecting the diffusion in the x-direction. When the penetration depth of the solute into the water is small compared to the distance along the path the error introduced is small. When the penetration depth of the solute is large and reaches the rock wall most of the water will be equilibrated and longitudinal diffusion will not further influence the solute transfer. The errors introduced are deemed be marginal considering the geometrical simplifications and other assumptions. The merit of the simplifications is that some very simple analytical expressions can be derived suitable for stochastic simulations. The simple expressions also give a good insight into the dominating mechanisms and parameters.

The equations to solve are

$$\frac{\partial c}{\partial t_{res}} = D_w\frac{\partial^2 c}{\partial y^2}$$

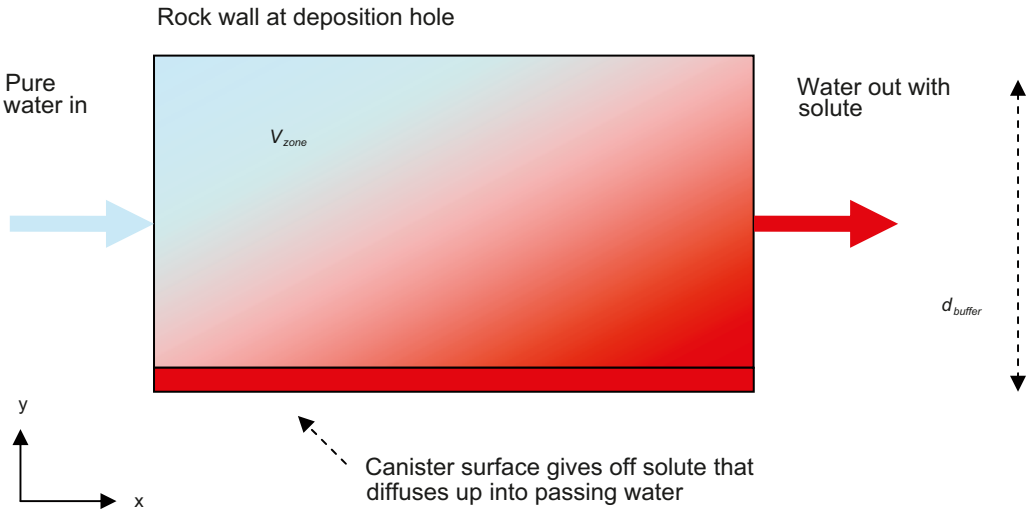

Figure A1. *Water flowing through the eroded buffer is contaminated by a solute released from the canister surface.*

With initial and boundary conditions

$c = 0 \quad at \quad t_{res} = 0$

$c = c_o \quad at \quad y = 0$

$$\frac{dc}{dy} = 0 \quad at \quad y = d_{buffer}$$

The solution is /Bird et al. p 377/[2]

$$\frac{c}{c_o} = 1 - 2\sum_{n=0}^{\infty} \frac{(-1)^n}{(n+1/2)\pi} e^{-\frac{(n+1/2)^2 \pi^2 D_w t_{res}}{d_{buffer}^2}} Cos((n+1/2)\frac{\pi y}{d_{buffer}}$$

The mean concentration c_{mean} is obtained by integration over the distance from y=0 to $y=d_{buffer}$

$$\frac{c_{mean}}{c_o} = (1 - 2\sum_{n=0}^{\infty} \frac{1}{(n+1/2)^2 \pi^2} e^{-\frac{(n+1/2)^2 \pi^2 D_w t_{res}}{d_{Buffer}^2}})$$

We wish to model how much solute, N, will be carried by a stream with flowrate q i.e.

$N = Q_{eq} * c_o = q * c_{mean}$

we want an expression for

$$Q_{eq} = q * \frac{c_{mean}}{c_o}$$

Using the expression for c_{mean} above leads to difficulties because the convergence of the infinite series is very slow for small $\frac{D_w t_{res}}{d_{buffer}^2}$ (high flowrate). However, for small $\frac{D_w t_{res}}{d_{Buffer}^2}$ c_{mean} is well approximated by /Bird et al. p 375–377/

$$\frac{c_{mean}}{c_o} = \frac{\eta_{mean}}{d_{Buffer}} = \frac{1.13\sqrt{D_w t_{res}}}{d_{Buffer}}$$

But $\frac{\eta_{mean}}{d_{Buffer}}$ must be smaller than 1 by some margin, otherwise we would predict a mean concentration larger than 1. Obviously for small q all the water will be equilibrated to c_o and Q_{eq} will be equal to q.

The value of q at which Q_{eq}=q is assessed by finding at what q_{lim} this is true. This is found at

$$q_{\lim} = 1.13^2 \frac{V_{zone} D_w}{d_{buffer}^2}$$

Thus a simple method to determine $Q_{eq}(q)$ is as follows

For $q > q_{lim}$ $\quad Q_{eq} = q \; 1.13\frac{\sqrt{D_w t_{res}}}{d_{buffer}} = 1.13\frac{\sqrt{q D_w V_{zone}}}{d_{buffer}}$

else $\quad Q_{eq} = q$

At q_{lim}, Q_{eq}=q=$1.2769\frac{V_{zone} D_w}{d_{buffer}^2}$

Figure A2 below, shows a plot of Q_{eq} and q vs q normalized with $\frac{V_{zone} D_w}{d_{buffer}^2}$=1. The two curves intersect at q=1.2769.

[2] Bird R B, Stewart W E, Lightfoot E N, 2002 Transport Phenomena 2nd Ed. John Wiley & Sons Inc. NY.

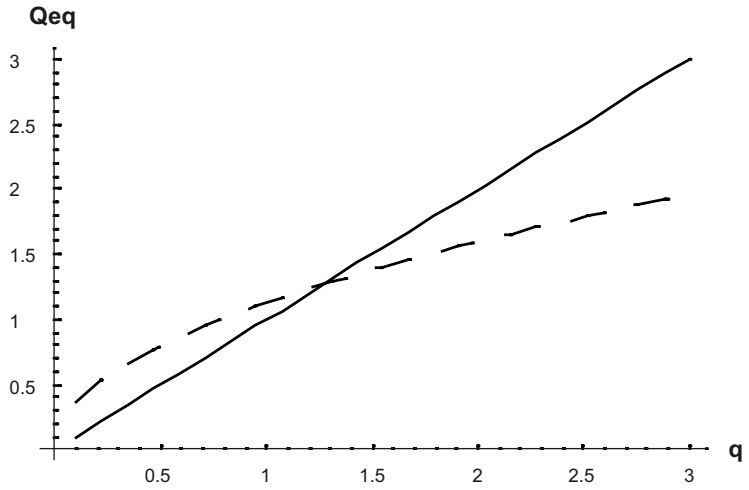

Figure A2. *Q_{eq} from the square root approximation, dashed curve, valid for large q's and Q_{eq}=q valid for small q's straight line.*

Figure A3 also shows the "exact" solution from the infinite series, dot-dashed curve, for comparison. The error using the approximations is at most 13 % in the vicinity of $q=q_{lim}$. The error is on the conservative side overestimating Q_{eq} and is deemed acceptable considering other approximations and the (considerable) savings in computer time.

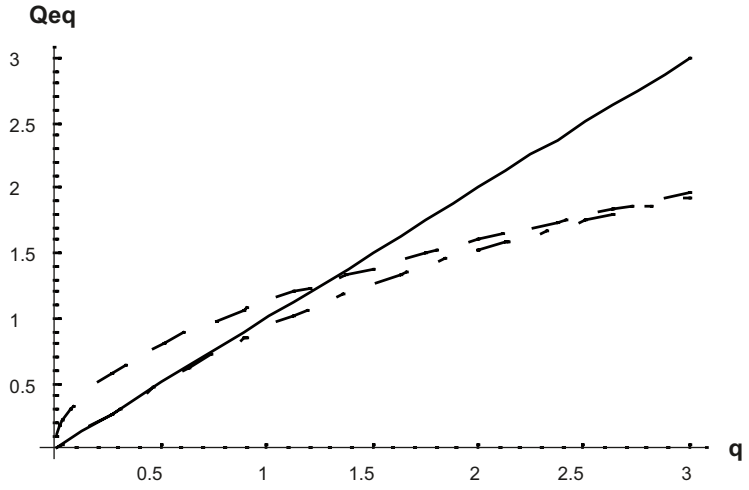

Figure A3. *Q_{eq} from the square root approximation q, dashed curve, valid for large q's and Q_{eq}=q valid for small q's straight line. Exact solution dot-dashed curve.*